

This is the peer reviewed version of the following article:

Proteomic analysis of two populations of *Schistosoma mansoni*-derived extracellular vesicles: 15k pellet and 120k pellet vesicles

Desalegn Woldeyohannes Kifle , Mark S Pearson, Luke Becker, Darren Pickering, Alex Loukas, Javier Sotillo

Mol Biochem Parasitol 2020 Mar;236:111264.

which has been published in final form at

<https://doi.org/10.1016/j.molbiopara.2020.111264>

1 **Proteomic analysis of two populations of *Schistosoma mansoni*-derived**
2 **extracellular vesicles: 15k pellet and 120k pellet vesicles**

3 Desalegn Woldeyohannes Kifle^{a,b}, Mark S. Pearson^a, Luke Becker^a, Darren Pickering^a,
4 Alex Loukas^{a*}, Javier Sotillo^{a,c*}

5 **Author affiliations**

6 ^aCentre for Molecular Therapeutics, Australian Institute of Tropical Health and
7 Medicine, James Cook University, Cairns, 4878, Queensland, Australia;

8 ^bAklilu Lemma Institute of Pathobiology, Addis Ababa University, 1176, Addis Ababa,
9 Ethiopia

10 ^cCentro Nacional de Microbiología, Instituto de Salud Carlos III, Majadahonda, Madrid,
11 Spain

12

13 *Corresponding authors:

14 Alex Loukas: alex.loukas@jcu.edu.au

15 Javier Sotillo: javier.sotillo@isci.es

16

17

18

19

20

21

22 **Abstract**

23 Helminth parasites secrete extracellular vesicles (EVs) into their environment that have
24 potential roles in host-parasite communication, and thus represent potentially useful
25 targets for novel control strategies. Here, we carried out a comprehensive proteomic
26 analysis of two different populations of EVs – 15k pellet and 120k pellet EVs – from
27 *Schistosoma mansoni* adult worms. We characterised the proteins present in the
28 membranes of the EVs (including external trypsin-liberated peptides, integral membrane
29 proteins (IMPs) and peripheral membrane proteins (PMPs)), as well as cargo proteins,
30 using LC-MS/MS. A total of 286 and 716 proteins were identified in 15k and 120k
31 pellets, respectively. Some of the most abundant proteins identified from both 15k and
32 120k pellets include known vaccine candidates such as *Sm*-TSP-2, saponin B domain-
33 containing proteins, calpain glutathione-S-transferase, Sm29 and cathepsin domain-
34 containing proteins. Other abundant proteins that have not been tested as vaccines
35 include DM9 domain-containing protein, 13kDa tegumental antigen and histone H4-like
36 protein. Sm23, a member of the tetraspanin family with known vaccine efficacy, was
37 identified in the cargo and IMP compartments of only 15k pellet vesicles. Moreover, a
38 collection of proteins with known or potential relevance in host-parasite communication
39 including proteases, antioxidants and EV biogenesis/trafficking of both vesicle types
40 were identified. Our results provide the first report of a comprehensive compartmental
41 proteomic analysis of adult *S. mansoni*-derived EVs. Future research should investigate
42 recombinant forms of these proteins as vaccine and serodiagnostic antigens as well as
43 the roles of EV proteins in host-parasite communication.

44

45 **Keywords:** *Schistosoma mansoni*, extracellular vesicles, 15k pellet extracellular
46 vesicles, 120k pellet extracellular vesicles, proteomics

48 **Abbreviations**

49 EVs: extracellular vesicles

50 GST: glutathione-S-transferase

51 HSP: heat shock protein

52 IMPs: integral membrane proteins

53 MVBs: multivesicular bodies

54 PMPs: peripheral membrane proteins

55 TLPs: trypsin liberated proteins

56 TSPs: tetraspanins

57 TRPS: tunable resistive pulse sensing

58

59

60 1. Introduction

61 Schistosomiasis is one of the most important parasitic helminth infections, affecting
62 nearly 240 million people worldwide, mainly in the tropics (1). Greater than 90% of the
63 infections occur in Africa and, of these, the majority are due to either *Schistosoma*
64 *mansoni* or *Schistosoma haematobium*, or both (2). Despite the use of mass drug
65 administration with praziquantel to treat schistosomiasis over the last two decades, the
66 infection still causes a loss of 1.53 million disability-adjusted life years. Indeed, in sub-
67 Saharan Africa alone, up to 280,000 deaths every year are attributable to
68 schistosomiasis (3).

69 Adult flukes possess a unique tegumental double bilayer, endowed with a population of
70 stem cells that undergoes frequent regeneration and turnover, which is instrumental in
71 immune escape pathways by making *S. mansoni* surface proteins inaccessible to host
72 immune cells (4). Currently, there is no vaccine available for schistosomiasis and
73 moreover, its treatment relies solely on a single drug, praziquantel, which warrants
74 concern about emerging drug resistance (5) and emphasises the need for rigorous
75 research into new drug targets and vaccine antigen discovery.

76 Schistosomiasis vaccine and diagnostic antigen discovery has focused on several
77 developmental stages of the parasite with an emphasis on the tegument and
78 excretory/secretory (ES) proteomes (6-13). Despite advances in the characterization of
79 the secretome, substantially less is known about the molecular mechanisms involved in
80 the release of these molecules. One such pathway is the release of extracellular vesicles
81 (EVs) which have been recently described in *S. mansoni* (14, 15) and other *Schistosoma*
82 spp. (16-18). EVs are membrane-enclosed vesicles that are continually secreted by
83 different types of cells in disease and normal states (19). EVs usually include apoptotic
84 bodies (originating from dying cells), microvesicles (MVs) (originating from plasma

85 membrane budding), and exosomes (released from multivesicular bodies). MVs and
86 exosomes are the best characterized types of EVs (19) in terms of morphology, size and
87 molecular composition (20). Several studies have demonstrated that parasite-derived
88 EVs play a key role during helminth infections. For example, EVs are capable of
89 modulating host innate immune responses (16, 21). In addition, the administration of
90 exosomes to mice primes the immune response and reduces the severity of clinical signs
91 in *Echinostoma caproni* infection (22). Moreover, immune reactivity towards
92 *Schistosoma japonicum* EVs was identified when using sera from *S. japonicum*-infected
93 rabbits (17). A recent study (23) demonstrated that, in a hamster vaccination-challenge
94 model, secreted EVs from *Opisthorchis viverrini* and recombinant versions of EV
95 surface tetraspanins (TSPs) induced antibody responses that resulted in significantly
96 reduced adult worm burdens after challenge infection. These findings serve as a
97 baseline for the identification of potential target molecules for the development of
98 schistosomiasis biomarkers and vaccines derived from EVs.

99 While the protein composition of schistosome EVs has been characterized at a crude,
100 whole-vesicle level, the sub-vesicular distribution of those proteins has not been
101 described. Herein, to our knowledge for the first time, we characterise the
102 compartmental proteome content of *S. mansoni*-derived small EVs (120k pellet), and
103 describe for the first time the presence of a relatively large schistosome EV (15k pellet)
104 population and its proteome.

105

106 **2. Material and methods**

107 **2.1 Ethics statement**

108 The study obtained ethical approval (A2004, A2391 and A2395) from the Animal
109 Ethics Committee at James Cook University. All studies involving mice were
110 performed at the animal facilities of the Australian Institute of Tropical Health and
111 Medicine in accordance with guidelines and protocols approved by the Animal Ethics
112 Committee.

113

114 **2.2 Mice and parasite material**

115 Male 6-8 week old BALB/c mice were used for the study. All animals were maintained
116 under standard conditions with food and water *ad libitum*. *S. mansoni* (Puerto Rican
117 strain)-infected *Biomphalaria glabrata* snails were provided by the National Institute of
118 Allergy and Infectious Diseases Schistosomiasis Resource Centre for distribution
119 through the Biodefense and Emerging Infections Research Resources Repository,
120 NIAID, National Institutes of Health, USA: *S. mansoni*, Strain NMRI; exposed *B.*
121 *glabrata*, NR-21962.

122

123 **2.3 Parasite culture and collection of excretory/secretory products**

124 To harvest ES products, *S. mansoni* adult worms were obtained from infected mice as
125 described previously (24). Briefly, mice were euthanized using an intraperitoneal
126 injection of 0.2 ml pentobarbital/heparin solution followed by CO₂ gas administration
127 and worms were perfused using perfusion solution (0.15 M sodium chloride with 0.03
128 M sodium citrate dehydrate in water) and collected in a container (24). Worms were
129 washed three times using serum-free Basch media (0.5 μM hypoxanthine (Sigma), 1
130 μM serotonin (Sigma), 1 μM hydrocortisone (Sigma), 0.2 μM triiodothyronine
131 (Calbiochem), 8 mg insulin (Lifetech), 0.5× MEM vitamin (Invitrogen), 2×

132 antibiotic/antimicotic (Invitrogen), 50 ml Schneider Drosophila medium (Invitrogen),
133 0.01 M HEPES (Invitrogen), and Eagle's basal medium (Invitrogen) to make 1 L final
134 volume) (25) and cultured for 3 h at 37°C with 5% CO₂ in serum-free Basch media with
135 a density of approximately 50 worm pairs in 5 ml of media. The culture media was
136 discarded after 3 h, and replaced with fresh culture media. Worms were cultured for a
137 further 10 days and ES products were collected every 24 h, centrifuged at 4°C (500 g,
138 2,000 g and 4,000 g for 30 min each) to pellet and discard parasite material such as
139 tegumental debris and eggs, and kept at -80°C until further analysis. Worms were
140 observed by microscopy daily to ensure that all were motile during *in vitro* culture.
141 Immotile worms were removed as soon as they were detected.

142

143 **2.4 EV isolation**

144 EVs were isolated and purified following established methods previously described for
145 *S. mansoni* (14). After differential centrifugation, samples were concentrated using a 10
146 kDa spin concentrator (Merck Millipore), and centrifuged at 15,000 g for 1 h at 4°C to
147 pellet 15k vesicles, which were washed with PBS three more times and kept at -80°C
148 until use. To collect 120k vesicles, supernatant was ultracentrifuged using an MLS-50
149 rotor (Beckman Coulter) at 120,000 g for 3 h at 4°C, and the resultant pellet was
150 resuspended in 200 µl of PBS and subjected to Optiprep® discontinuous gradient
151 separation. One ml of 40%, 20%, 10% and 5% iodixanol solutions prepared in 10 mM
152 Tris-HCl, 0.25 M sucrose, pH 7.2, was layered in decreasing density using an
153 ultracentrifuge tube, and the 200 µl containing the resuspended EVs was added to the
154 top layer and ultracentrifuged at 120,000 g for 18 h at 4°C. A control tube was prepared
155 in a similar way, replacing EVs with PBS to calculate the density of fractions. A total of

156 12 sample fractions were collected from the Optiprep® discontinuous gradient, and the
157 excess Optiprep® solution was buffer exchanged using PBS containing 1× EDTA-free
158 protease inhibitor cocktail (Santa Cruz, Dallas, TX, USA) using a 10 kDa spin
159 concentrator. The absorbance was measured at 340 nm for each fraction obtained from
160 the control tubes, and their densities were calculated. Finally, protein concentration of
161 all sample fractions was measured using a Bradford Protein Assay Kit (ThermoFisher).

162

163 **2.5 Tunable Resistive Pulse Sensing analysis of EVs**

164 The particle concentration and size distribution of each fraction was analysed for both *S.*
165 *mansoni*-derived 120k and 15k vesicle pellets by tunable resistive pulse sensing
166 (TRPS) using a qNano instrument (Izon) following the manufacturer's instructions.
167 120k pellet vesicles from four different cultures were analysed using TRPS, and all
168 fractions containing 120k vesicles (based on specific gravity/density analysis) from
169 eight batches were pooled together. Finally, TRPS analysis was carried out again on the
170 pooled sample before proteomic analysis was conducted. TRPS, concentration and
171 purity analysis, was performed on the pooled 15k pellet sample isolated from eight
172 different batches of cultured worms. Nanopore NP150 and NP300 were used for 120k
173 and 15k vesicle pellets, respectively. Pressure and voltage values were set to optimize
174 the signal to ensure high sensitivity. Samples were diluted 1:5 in electrolyte (Izon)
175 before applying to the nanopore. Calibration was performed using CP100 and CP400
176 carboxylated polystyrene calibration particles (Izon) for 120k and 15k vesicle pellets,
177 respectively, at a 1:2,000 dilution. Size distribution and concentration of particles were
178 analyzed using the software provided by Izon (version 3.2). Purity analysis of both

179 ELVs and MVs (number of particles/ μg of protein) was performed following methods
180 described by Webber and Clayton (26).

181

182 **2.6 Trypsin shaving and sequential protein extraction of purified *S. mansoni* EVs**

183 Peptides from surface-accessible proteins were released by trypsin hydrolysis of EVs
184 using a protocol described previously (27). Briefly, sequencing-grade trypsin (1 $\mu\text{g}/\mu\text{l}$)
185 was added to purified EVs for 10 min at 37°C. Treated EVs were then centrifuged at
186 120,000 g at 4°C for 1 h, and surface peptides were obtained from the supernatant. EVs
187 collected as a pellet were further processed to investigate proteins associated with the
188 EV membrane and within the EV lumen. Briefly, EVs were resuspended in water and
189 sonicated (3x) which resulted in the release of EV cargo content which was recovered
190 from the supernatant by centrifugation at 120,000 g for 1 h at 4°C. Subsequently, the
191 pellet was incubated with 0.1 M Na_2CO_3 (pH 11) on ice for 30 min and then centrifuged
192 at 120,000 g at 4°C for 1 h to recover peripheral membrane proteins (PMPs) from the
193 supernatant. Finally, integral membrane proteins (IMPs) were obtained by solubilizing
194 the pellet in 1% Triton X-100/2% sodium dodecyl sulphate (SDS) at 37°C for 15 min.

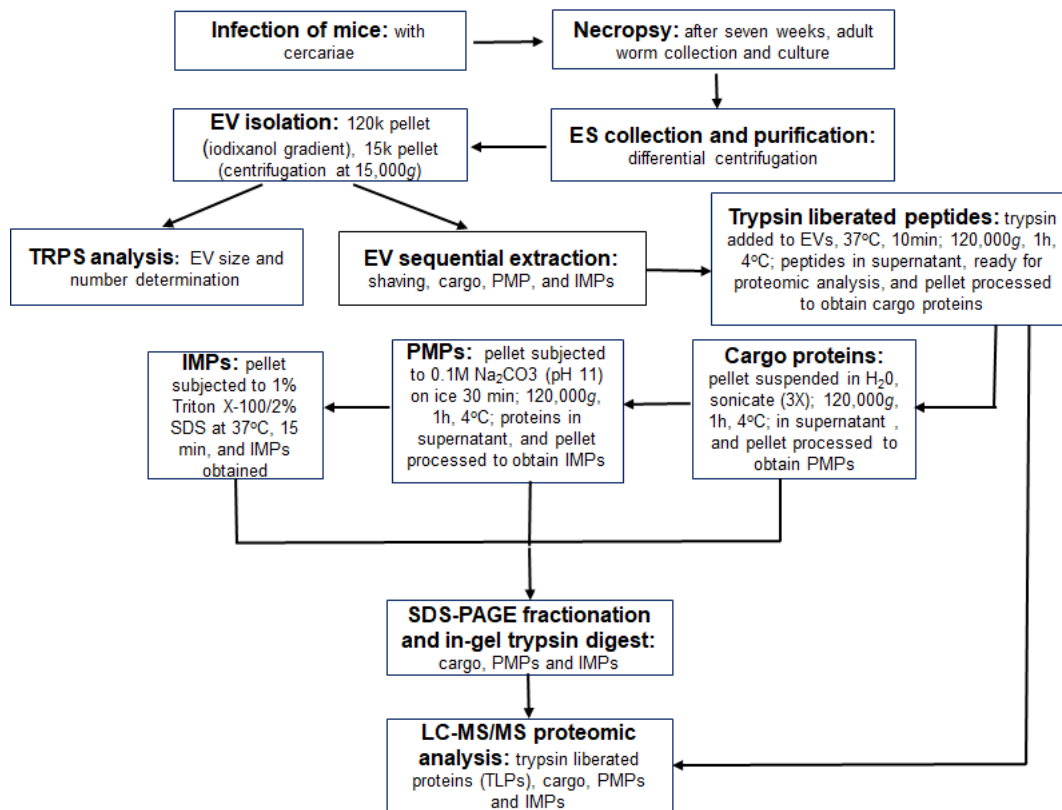
195

196 **2.7 In-gel digestion of proteins**

197 For the proteomic analysis, each separated component of cargo, integral membrane and
198 peripheral membrane proteins were electrophoresed on a 10% SDS-PAGE gel for 60
199 min at 140 V. Tryptic in-gel digestion was performed as described previously with
200 minor modifications (28). In brief, the gel was stained with Coomassie blue (0.03%),
201 destained overnight and each lane was cut into 7 slices (approximately 1 mm^2). Each
202 band was destained by washing twice in 50% acetonitrile with 200 mM ammonium

203 bicarbonate at 37°C for 45 min, reduced with 20 mM dithiothreitol (Sigma) in 25 mM
 204 ammonium bicarbonate for 1 h at 65°C, alkylated with 50 mM iodoacetamide (IAM,
 205 Sigma) in 25 mM ammonium bicarbonate at 37°C for 15 min and digested with 100
 206 ng/μl trypsin (Sigma) at 37°C for 18 h. Peptides were extracted in 50% acetonitrile with
 207 0.1% trifluoroacetic acid. The last step was performed three times to maximize peptide
 208 recovery. All peptides were finally dried in a vacuum concentrator. Samples were then
 209 resuspended in 10 μl of 0.1% trifluoroacetic acid and tryptic peptides were desalted
 210 using a Zip-Tip® column (Merck Millipore) pipette tip according to manufacturer's
 211 protocol and dried in a vacuum concentrator before analysis using liquid
 212 chromatography-tandem mass spectrometry (LC-MS/MS). The experimental work-flow
 213 from sample collection to proteomic analysis is shown in Figure 1.

214



215

216

217 **Figure 1. Overview of experimental workflow for proteomic analysis of *S.***
218 ***mansoni*-derived EVs.** Seven weeks after infection of mice with *S. mansoni* cercariae,
219 adult worms were perfused and cultured. Excretory/secretory (ES) products were
220 collected and purified from cell-conditioned media using differential centrifugation (500
221 g, 2,000 g and 4,000 g at 4°C, each for 30 min), followed by ultracentrifugation at
222 15,000 g at 4°C for 1 h to pellet 15k pellet vesicles . The supernatant was then subjected
223 to ultracentrifugation at 120,000 g at 4°C for 3 h to pellet the 120k pellet vesicles. The
224 purity and concentration of 120k vesicles were enhanced using an Optiprep® gradient.
225 Size and concentration of EVs were determined by tunable resistive pulse sensing using
226 a qNano instrument. For the proteomic analysis, EV surface-exposed proteins were
227 obtained using trypsin shaving, then, sequential extraction resulted in purification of
228 cargo proteins, PMPs and IMPs. Proteins were submitted to in-gel trypsin digestion and
229 LC-MS/MS for proteomic analysis.

230

231 **2.8 LC-MS/MS protein analysis**

232 Tryptic fragments from each sample were resuspended in 8 µl of 0.1 % formic acid in
233 LC-MS/MS-grade water and separated chromatographically by an Eksigent nanoLC
234 415 system using a 15 cm long Eksigent column (C18-CL particle size 3 µm, 120 Å, 75
235 µm ID) and a linear gradient of 3-40% solvent B (100 acetonitrile/0.1% formic acid
236 [aq]) for 45 min followed by 40-80 % solvent B in 5 min. A pre-concentration step (10
237 min) was performed employing an Eksigent Trap-column (C18-CL, 3 µm, 120 Å, 350
238 µm x 0.5 mm) before commencement of the gradient. A flow rate of 300 nl/min was
239 used for all experiments. The mobile phase consisted of solvent A (0.1% formic acid
240 [aq]) and solvent B. Eluates from the RP-HPLC column were directly introduced into
241 the PicoView ESI ionisation source of a TripleTOF 6600 MS/MS System (AB Sciex)

242 operated in positive ion electrospray mode. All analyses were performed using
243 Information Dependant Acquisition. AnalystTF 1.7.1 (Applied Biosystems) was used
244 for data analysis. Briefly, the acquisition protocol consisted of the use of an Enhanced
245 Mass Spectrum scan with 15 sec exclusion time and 100 ppm mass tolerance. A cycle
246 time of 1800 ms was used to acquire full scan TOF-MS data over the mass range 400–
247 1250 m/z and product ion scans over the mass range of 100–1500 m/z for up to 30 of
248 the most abundant ions with a relative intensity above 150 and a charge state of +2 – +5.
249 Full product ion spectra for each of the selected precursors were then used for
250 subsequent database searches.

251

252

253 **2.9 Database search and protein sequence analysis**

254 Data were searched against a database comprising the *S. mansoni* proteome obtained
255 from WormBase ParaSite (<http://parasite.wormbase.org/>) appended to the common
256 Repository of Adventitious Proteins (cRAP; <http://www.thegpm.org/crap/>) and their
257 reversed decoy sequences using SearchGUI (v3.3.5). X!Tandem (vAlanin), Comet
258 (v2018.01 rev.2), Tide (v3.2.x), MyriMatch (v2.1) and MS-GF + (v2016.01.02) were
259 the search engines used, and the identification results were validated using
260 PeptideShaker (v1.16.31). All searches were conducted employing the following search
261 parameters: trypsin as digestion enzyme, maximum missed cleavages, 2; precursor ion
262 mass tolerance \pm 10 ppm, fragment ion tolerance \pm 0.1 Da; fixed modifications:
263 carbamidomethylation of cysteine; variable modifications: deamidation of asparagine
264 and glutamine, oxidation of methionine; Peptide Spectrum Matches (PSMs), peptides
265 and proteins were validated at a 1.0% False Discovery Rate estimated using the decoy

266 hit distribution. Reported results correspond to those proteins showing ≥ 2 distinct
267 unique peptides. An estimate of the relative abundance of the predicted proteins was
268 assessed using the spectrum counting abundance index (29). The mass spectrometry
269 proteomics data have been deposited to the ProteomeXchange Consortium via the
270 PRIDE partner repository with the dataset identifier PXD015857 and
271 10.6019/PXD015857.

272

273 **2.10 Bioinformatic analyses**

274 Gene ontology (GO) annotations were obtained using the Blast2GO software (30), and
275 GO terms were assigned as biological process or molecular function. Only children GO
276 terms were used for subsequent analysis to avoid redundancy in GO terms. REViGO
277 was used to summarize and plot GO terms (31). Protein family (Pfam) analysis was
278 performed at the E-value <0.05 threshold using HMMER software (30). Signal peptides
279 and transmembrane domains were predicted using SignalP v4.1 and TMHMM v2.0,
280 respectively (32, 33).

281

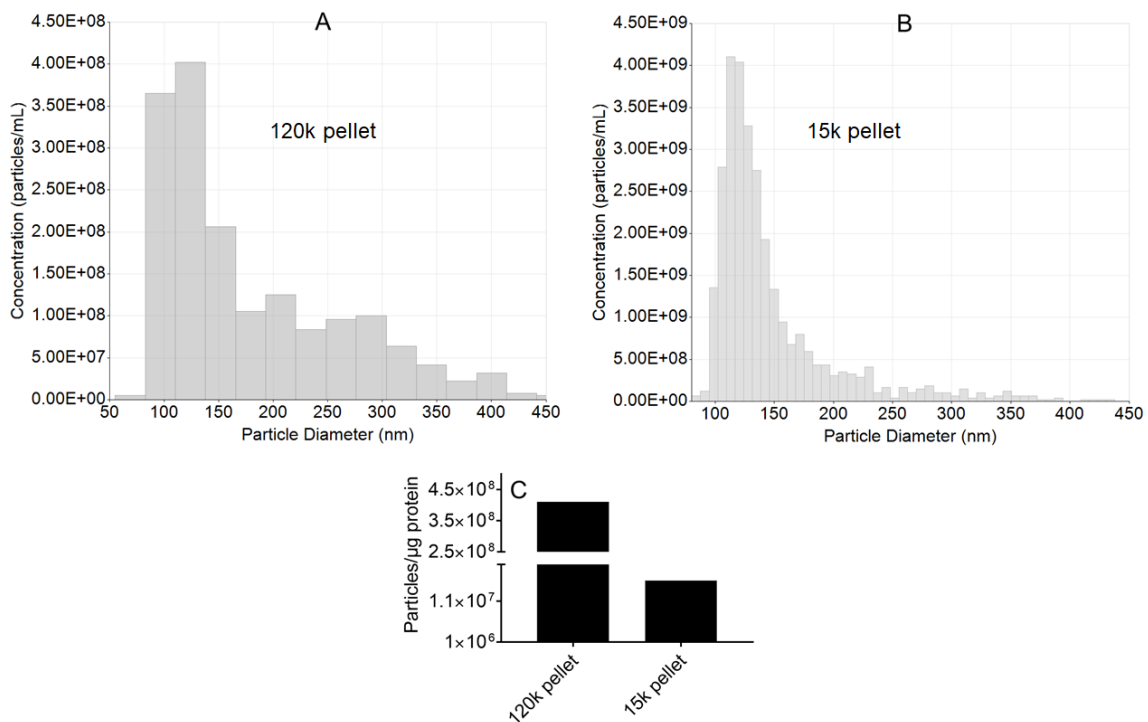
282 **3. Results**

283 **3.1 EV size, concentration and purity**

284 *S. mansoni* adult worm-derived ELVs were purified using an iodixanol density gradient
285 as described previously for other helminths (14, 34, 35). The density and protein
286 concentration of all 12 fractions collected from the gradient were analysed. Fractions of
287 120k pellet vesicles from different batches with densities ranging from 1.09 to 1.22 g/ml
288 (fractions containing *S. mansoni* small vesicles) as described previously (14) were
289 combined and subjected to TRPS analysis using a qNano instrument to determine size

290 and concentration of 120k vesicles (Figure 2A). Likewise, 15k pellet vesicles collected
291 from different batches of EVs were combined, protein concentration was measured and
292 TRPS analysis was performed to obtain size and concentration (Figure 2B) of 15k
293 vesicles-enriched sample. Accordingly, purity analysis of both 120k (4.1×10^8
294 particles/ μg protein) and 15k pellet vesicles (1.6×10^7 particles/ μg protein) (Figure 2C)
295 was also performed as described previously (26).

296
297
298
299

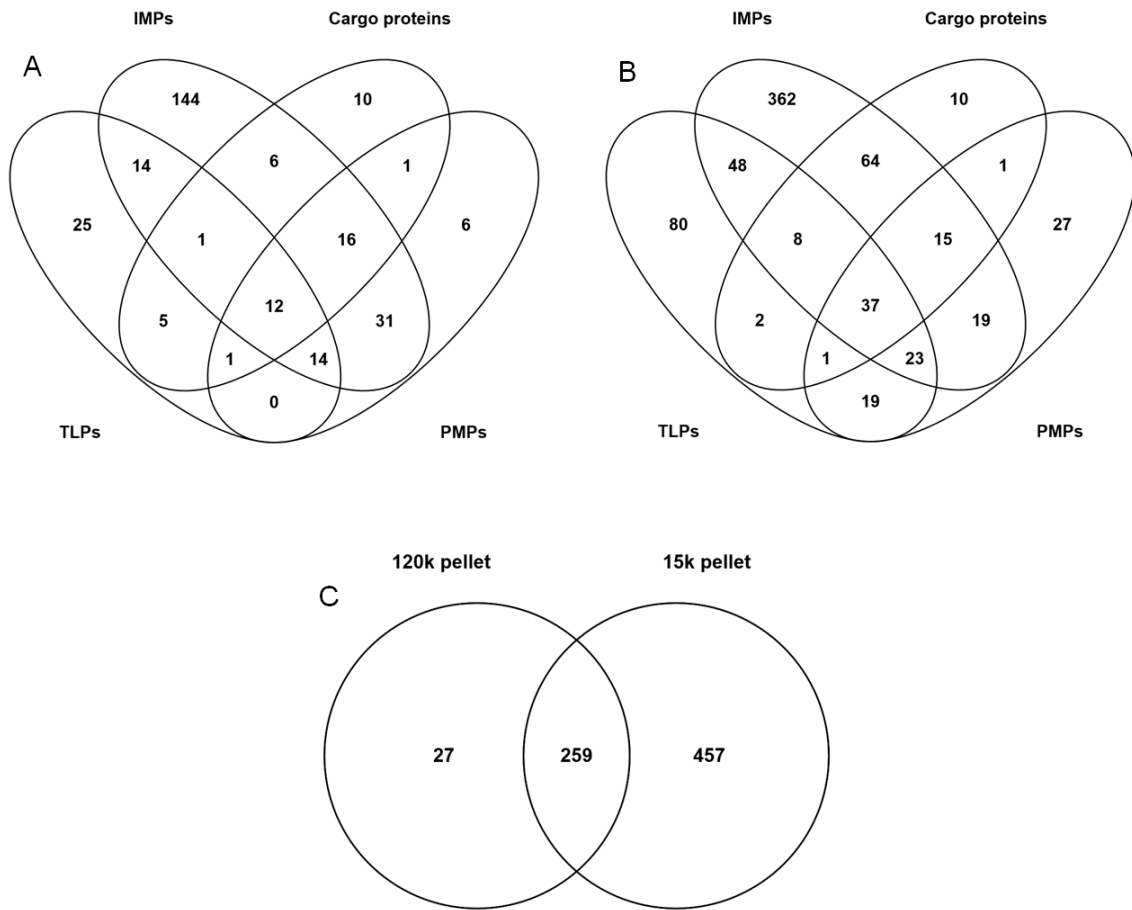


300
301
302
303
304
305
306

Figure 2. Tunable resistive pulse sensing (TRPS) analysis and purity on *S. mansoni*-driven extracellular vesicles. Particle size (x-axis) and number (y-axis) of 120k pellet (A) and 15k pellet vesicles (B) after purification were analysed by TRPS using a qNano instrument (iZon). The purity of both 120k and 15k pellet vesicles (C) was determined according to Webber and Clayton (26).

307 **3.2 Proteomic analysis of *S. mansoni*-derived EVs**

308 A proteomic analysis on each of the four components - TLPs, cargo proteins, IMPs and
309 PMPs - of both 120k and 15k pellet vesicles was performed. In total, 286 and 716
310 different proteins were identified from *S. mansoni*-derived 120k (Figure 3A) and 15k
311 pellet vesicles (Figure 3B), respectively. Of these, 27 were specific to 120k pellet and
312 457 specific to 15k pellet vesicles, while 259 proteins were identified in both types of
313 EVs (Figure 3C). Antioxidants such as peroxiredoxin (Prx3) and proteins involved in
314 exosome biogenesis or trafficking, such as vacuolar protein sorting-associated protein
315 28 homolog, were among the 27 120k vesicle-specific proteins identified (Table 1,
316 Figure 4). 120k pellet vesicles contained 72 TLPs (Supplementary Table S1), 52 cargo
317 proteins (Supplementary Table S2), 238 proteins in the IMP component (Supplementary
318 Table S3) and 81 proteins in the PMP component (Supplementary Table S4). 15k pellet
319 vesicles, on the other hand, contained 218 TLPs (Supplementary Table S5), 138 cargo
320 proteins (Supplementary Table S6), 576 IMPs (Supplementary Table S7) and 142 PMPs
321 (Supplementary Table S8). Some of the most abundant proteins identified, based on
322 spectrum counting, in both *S. mansoni*-derived 120k (Supplementary Table S1-S4) and
323 15k pellet vesicles (Supplementary Table S5-S8), included the TSPs TSP-2 and TSP-4,
324 glutathione-S-transferase (GST), saponin B domain-containing protein, DM9 domain-
325 containing protein, cathepsin domain-containing proteins, 13 kDa tegumental antigen,
326 and histone H4-like protein. However, the TSP Sm23 was only identified in 15k pellet
327 vesicles.



328

329 **Figure 3. Shared and specific adult *S. mansoni*-derived EVs proteins.** Venn diagram
 330 representing the number of proteins identified from the four sub-vesicular components,
 331 enumerating specific and shared proteins of 120k pellet (A) and 15k pellet vesicles (B)
 332 and between the two vesicle types (C).

333

334

335

336

337

338

339

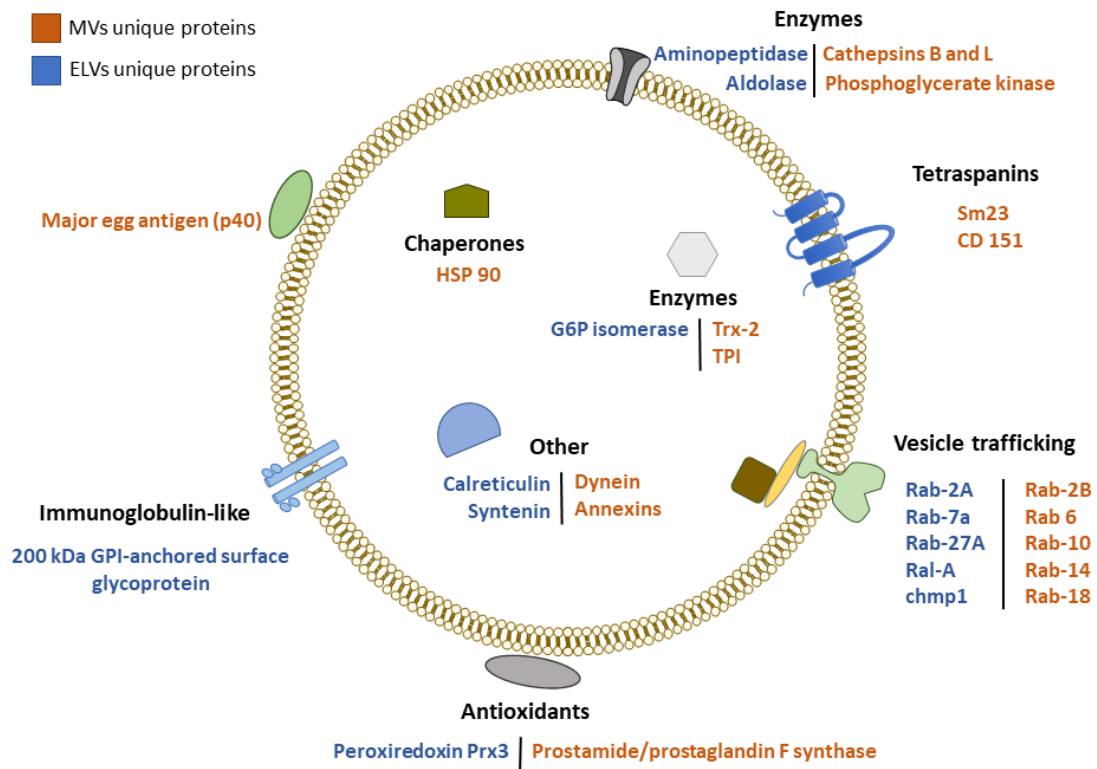
Table 1. Functional annotation of proteins from adult *S. mansoni*-derived 120k pellet vesicles.

| Accession number | Description | # Unique peptides | | | |
|------------------|---|-------------------|-------|------|------|
| | | TLPs | Cargo | IMPs | PMPs |
| | Proteases/inhibitors | | | | |
| Smp_032580.1 | subfamily T1A non-peptidase homologue (T01 family) | 2 | 4 | 0 | 0 |
| Smp_070930.1 | proteasome (prosome macropain) subunit alpha type 4 | 4 | 3 | 0 | 0 |
| Smp_034490.1 | Proteasome subunit beta type-6 | 0 | 2 | 0 | 0 |
| Smp_187140.1 | Cathepsin L-like proteinase precursor | 0 | 3 | 4 | 5 |
| Smp_301340.1 | proteasome (prosome, macropain) subunit, beta type,1 | 0 | 2 | 0 | 0 |
| Smp_214190.1 | Calpain | 4 | 4 | 11 | 3 |
| Smp_340060.1 | Mastin precursor | 0 | 6 | 9 | 8 |
| Smp_006390.1 | cysteine protease inhibitor | 0 | 0 | 3 | 0 |
| Smp_030000.1 | Putative aminopeptidase W07G4.4 | 10 | 0 | 7 | 0 |
| Smp_103610.1 | cathepsin B-like peptidase (C01 family) | 0 | 0 | 4 | 2 |
| Smp_343260.1 | cathepsin L, a | 3 | 0 | 7 | 3 |
| Smp_083870.1 | Putative aminopeptidase W07G4.4 | 4 | 0 | 0 | 0 |
| Smp_029500.1 | Thimet oligopeptidase | 2 | 0 | 0 | 0 |
| Smp_212920.1 | 20S proteasome subunit alpha 6 | 2 | 0 | 0 | 0 |
| Smp_207080.1 | Proteasome subunit alpha type-6 | 2 | 0 | 0 | 0 |
| Smp_089670.1 | Alpha-2-macroglobulin-like protein 1 | 5 | 35 | 0 | 2 |
| Smp_090080.1 | Estrogen-regulated protein EP45 precursor | 0 | 5 | 0 | 0 |
| Smp_075800.1 | hemoglobinase (C13 family) | 0 | 0 | 2 | 0 |
| Smp_007550.1 | Uncharacterized | 2 | 0 | 0 | 0 |
| | Biogenesis/vesicle trafficking | | | | |
| Smp_035620.1 | Multivesicular body subunit 12B | 0 | 0 | 3 | 0 |
| Smp_048940.1 | Vacuolar protein sorting-associated protein 37B | 0 | 0 | 3 | 0 |
| Smp_055880.1 | chmp1 (chromatin modifying protein) (charged multivesicular body protein), putative | 0 | 0 | 8 | 0 |
| Smp_067540.1 | Vacuolar protein sorting-associated protein 28 homolog | 0 | 0 | 2 | 0 |
| Smp_034870.1 | AP-2 complex subunit beta | 0 | 0 | 4 | 0 |
| Smp_055870.1 | vesicle-associated membrane protein 7-like | 0 | 2 | 11 | 2 |
| Smp_068530.1 | putative syntenin | 0 | 2 | 8 | 3 |
| Smp_074140.1 | Annexin A13 (Annexin XIII) | 3 | 4 | 13 | 9 |
| Smp_013690.1 | BRO1 domain-containing protein BROX | 3 | 0 | 16 | 9 |
| Smp_071630.1 | Ras-related protein Rab-2A | 0 | 0 | 6 | 0 |
| Smp_077720.1 | putative annexin | 0 | 0 | 6 | 5 |
| Smp_062300.1 | Ras-related C3 botulinum toxin substrate 1 | 0 | 0 | 3 | 0 |
| Smp_045550.1 | putative annexin | 0 | 0 | 11 | 0 |
| Smp_067140.1 | Ras-related protein Rab-7a | 0 | 0 | 2 | 0 |
| Smp_104670.1 | ras-related protein Rab-8A isoform X1 | 0 | 0 | 3 | 0 |

| | | | | | |
|---------------------------|---|---|----|----|----|
| Smp_139340.1 | Ras-related protein Rab-27A | 0 | 0 | 4 | 0 |
| Smp_094820.1 | Vacuolar protein sorting-associated protein VTA1-like protein | 0 | 0 | 4 | 0 |
| Smp_094420.1 | Rab GDP dissociation inhibitor alpha | 0 | 0 | 4 | 4 |
| Smp_210430.1 | Rab-protein 8 | 0 | 0 | 2 | 0 |
| Smp_104310.1 | rab11, putative | 0 | 0 | 7 | 0 |
| Smp_312770.1 | Ras-related protein Ral-A | 0 | 0 | 3 | 0 |
| Smp_045710.1 | Charged multivesicular body protein 4b | 0 | 0 | 6 | 0 |
| Antioxidants | | | | | |
| Smp_309480.1 | Uncharacterized | 2 | 2 | 4 | 0 |
| Smp_004470.1 | Peroxiredoxin, Prx3 | 2 | 0 | 0 | 0 |
| Smp_158110.1 | Thioredoxin peroxidase | 2 | 0 | 0 | 0 |
| Membrane structure | | | | | |
| Smp_040970.1 | putative vacuolar proton atpases | 0 | 2 | 23 | 5 |
| Smp_041460.1 | tetraspanin, putative (<i>Sm-TSP-D76</i>) | 0 | 7 | 9 | 7 |
| Smp_017730.1 | 200-kDa GPI-anchored surface glycoprotein | 7 | 14 | 0 | 0 |
| Smp_017430.1 | CD63 antigen | 0 | 5 | 9 | 5 |
| Smp_055780.1 | Multidrug resistance protein 1 | 4 | 4 | 50 | 24 |
| Smp_140000.1 | putative tetraspanin-CD63 receptor (<i>Sm-TSP-4</i>) | 0 | 3 | 7 | 4 |
| Smp_155310.1 | tetraspanin, putative (<i>Sm-TSP-1</i>) | 0 | 2 | 6 | 0 |
| Smp_104270.1 | Bis(5'-adenosyl)-triphosphatase enpp4 | 0 | 14 | 28 | 19 |
| Smp_313560.1 | alkaline phosphatase | 2 | 4 | 19 | 4 |
| Smp_344440.1 | putative tetraspanin 18, isoform 1 | 0 | 4 | 11 | 6 |
| Smp_015020.1 | Sodium/potassium-transporting ATPase subunit alpha | 0 | 0 | 11 | 0 |
| Smp_004310.1 | ATPase, H ⁺ transporting, lysosomal, V0 subunit c | 0 | 0 | 4 | 0 |
| Smp_005720.1 | Aquaporin-3 (AQP-3) | 0 | 0 | 2 | 0 |
| Smp_011560.1 | putative tetraspanin | 0 | 0 | 2 | 0 |
| Smp_042910.1 | osteopetrosis associated transmembrane protein | 0 | 0 | 2 | 0 |
| Smp_043990.1 | basigin related | 0 | 0 | 3 | 0 |
| Smp_037540.1 | putative alpha-amylase | 0 | 0 | 6 | 0 |
| Smp_032520.1 | putative lysosome-associated membrane glycoprotein | 0 | 0 | 3 | 0 |
| Smp_031880.1 | Immunoglobulin-like domain-containing protein | 0 | 0 | 3 | 0 |
| Smp_162510.1 | SJCHGC07463 protein | 0 | 0 | 6 | 0 |
| Smp_128110.1 | transporter, major intrinsic protein family protein | 0 | 0 | 2 | 0 |
| Smp_201730.1 | SJCHGC09800 protein | 0 | 0 | 2 | 0 |
| Smp_091650.1 | putative phospholipid-transporting ATPase IIB | 0 | 0 | 18 | 0 |
| Smp_153390.1 | putative ectonucleotide pyrophosphatase/phosphodiesterase | 0 | 0 | 2 | 0 |
| Smp_123280.1 | Major facilitator superfamily domain-containing protein 1 | 0 | 0 | 10 | 4 |
| Smp_244680.1 | protein VAC14 homolog | 0 | 0 | 2 | 0 |
| Smp_174490.1 | expressed conserved protein | 0 | 0 | 7 | 0 |

| | | | | | |
|--------------|---|---|---|----|---|
| Smp_169610.1 | putative zinc finger protein | 0 | 0 | 2 | 0 |
| Smp_159070.1 | hypothetical protein MS3_09367 | 0 | 0 | 2 | 0 |
| Smp_128940.1 | putative metabotropic glutamate receptor | 0 | 0 | 5 | 0 |
| Smp_131840.1 | 25 kDa integral membrane protein | 0 | 0 | 2 | 0 |
| Smp_169870.1 | putative cystinosin | 0 | 0 | 3 | 0 |
| Smp_095630.1 | CD9-like protein Sm-TSP-1 | 0 | 0 | 2 | 0 |
| Smp_130300.1 | Sodium/potassium-transporting ATPase subunit alpha | 0 | 0 | 4 | 0 |
| Smp_123670.1 | Lysosomal acid phosphatase | 0 | 0 | 4 | 2 |
| Smp_091240.1 | Voltage-dependent anion-selective channel protein 2 | 0 | 0 | 4 | 2 |
| Smp_165170.1 | putative transient receptor potential cation channel, subfamily m, member | 0 | 0 | 2 | 0 |
| Smp_150500.1 | Protein lifeguard 3 | 0 | 0 | 2 | 0 |
| Smp_167240.1 | SJCHGC05348 protein | 0 | 0 | 5 | 0 |
| Smp_210250.1 | CDC50 family protein, LEM3 family | 0 | 0 | 6 | 0 |
| Smp_089700.1 | integrin beta 2 | 0 | 0 | 4 | 0 |
| Smp_129820.1 | multi drug resistance-associated protein | 0 | 0 | 4 | 0 |
| Smp_166340.1 | SJCHGC03061 protein | 0 | 0 | 2 | 0 |
| Smp_147070.1 | Putative sodium-coupled neutral amino acid transporter 9 | 0 | 0 | 4 | 0 |
| Smp_160160.1 | putative sialin (solute carrier family 17 member 5) (sodium/sialic acid cotransporter) (ast) (membrane glycoprotein hp59) | 0 | 0 | 5 | 0 |
| Smp_162770.1 | lysosome-associated membrane glycoprotein | 0 | 0 | 3 | 0 |
| Smp_099150.1 | Pleckstrin homology domain-containing family B member 2 | 0 | 0 | 5 | 0 |
| Smp_194920.1 | T-cell immunomodulatory protein | 0 | 0 | 10 | 7 |
| Smp_164210.1 | Synaptosomal-associated protein 25 | 0 | 0 | 16 | 0 |
| Smp_246270.1 | ATP-binding cassette sub-family B member 6, mitochondrial | 0 | 0 | 16 | 7 |
| Smp_344430.1 | SID1 transmembrane family member 1 | 0 | 0 | 4 | 0 |
| Smp_302090.1 | putative ctl2 | 0 | 0 | 4 | 3 |
| Smp_267000.1 | ATPase, H ⁺ transporting, lysosomal accessory protein 1 | 0 | 0 | 7 | 3 |
| Smp_324850.1 | SJCHGC01860 protein | 0 | 0 | 3 | 0 |
| Smp_300190.1 | Aquaporin-9 (AQP-9) (Small solute channel 1) | 0 | 0 | 2 | 0 |
| Smp_340540.1 | lysosome membrane protein 2 | 0 | 0 | 5 | 2 |
| Smp_245370.1 | Equilibrative nucleoside transporter 3 | 0 | 0 | 3 | 0 |
| Smp_141010.1 | Dysferlin | 0 | 0 | 0 | 6 |
| Smp_335630.1 | tetraspanin 2 (<i>Sm-TSP-2</i>) | 0 | 5 | 6 | 6 |
| Smp_040080.1 | SJCHGC08990 protein | 0 | 0 | 7 | 5 |
| Smp_074140.1 | Annexin 13 | 0 | 0 | 4 | 0 |
| Smp_069120.1 | Synaptotagmin-2 | 0 | 0 | 2 | 0 |
| Smp_127820.1 | SJCHGC05417 protein | 0 | 0 | 2 | 0 |

344



345

346 **Figure 4. Schematic representation of most representative 120k and 15k pellet**
 347 **vesicle-unique proteins.** Several unique membrane and cargo specific proteins were
 348 found in the different populations of extracellular vesicles isolated from the
 349 excretory/secretory products of *Schistosoma mansoni*.

350

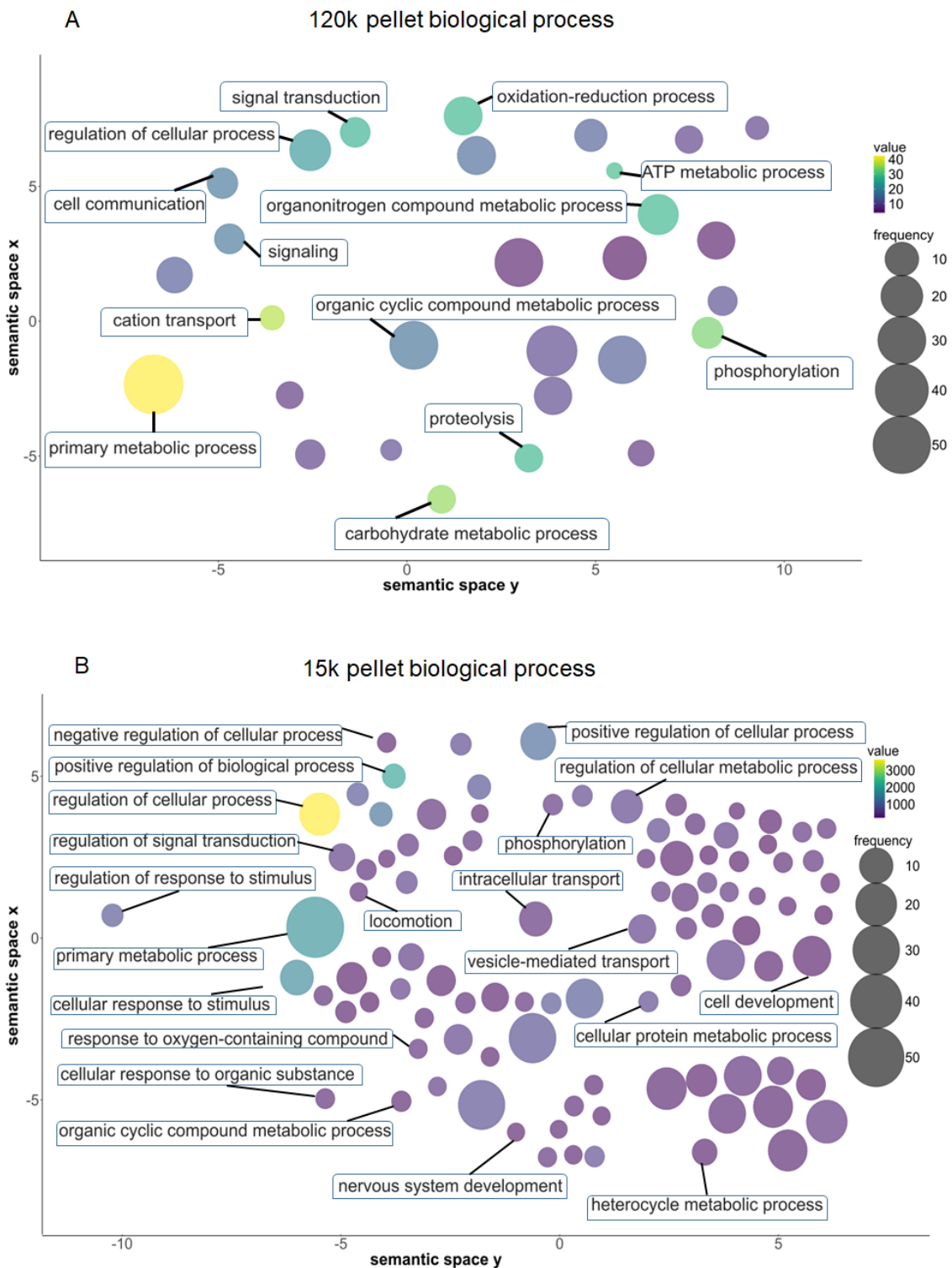
351

352 A GO and protein family analysis of the identified proteins from both *S. mansoni*-
 353 derived 120k and 15k pellets was performed. The most abundant GO terms within the
 354 “biological process” ontology of 120k pellet vesicles (Figure 5A) were “primary
 355 metabolic process” followed by “cation transport”, “carbohydrate metabolic process”,
 356 “phosphorylation” and “ATP metabolic process”; whereas the most abundant biological
 357 process GO terms for 15k vesicles (Figure 5B) were “regulation of cellular process”

358 followed by “positive regulation of biological process”, “primary metabolic process”,
359 “cellular response to stimuli”, and “positive regulation of cellular process”.

360 The most prominent GO terms within the “molecular function” ontology of 120k
361 vesicles (Figure 6A) were “protein binding” followed by “transmembrane transporter
362 activity”, “transferase activity”, and “oxidoreductase activity”; whereas the most
363 prominent molecular function GO terms for 15k pellet vesicles MVs (Figure 6B) were
364 “heterocyclic compound binding” followed by “anion binding”, “carbohydrate
365 derivative binding” and “cytoskeletal protein binding”.

366



367

368 **Figure 5. Bioinformatic analysis of gene ontology biological process terms in adult**

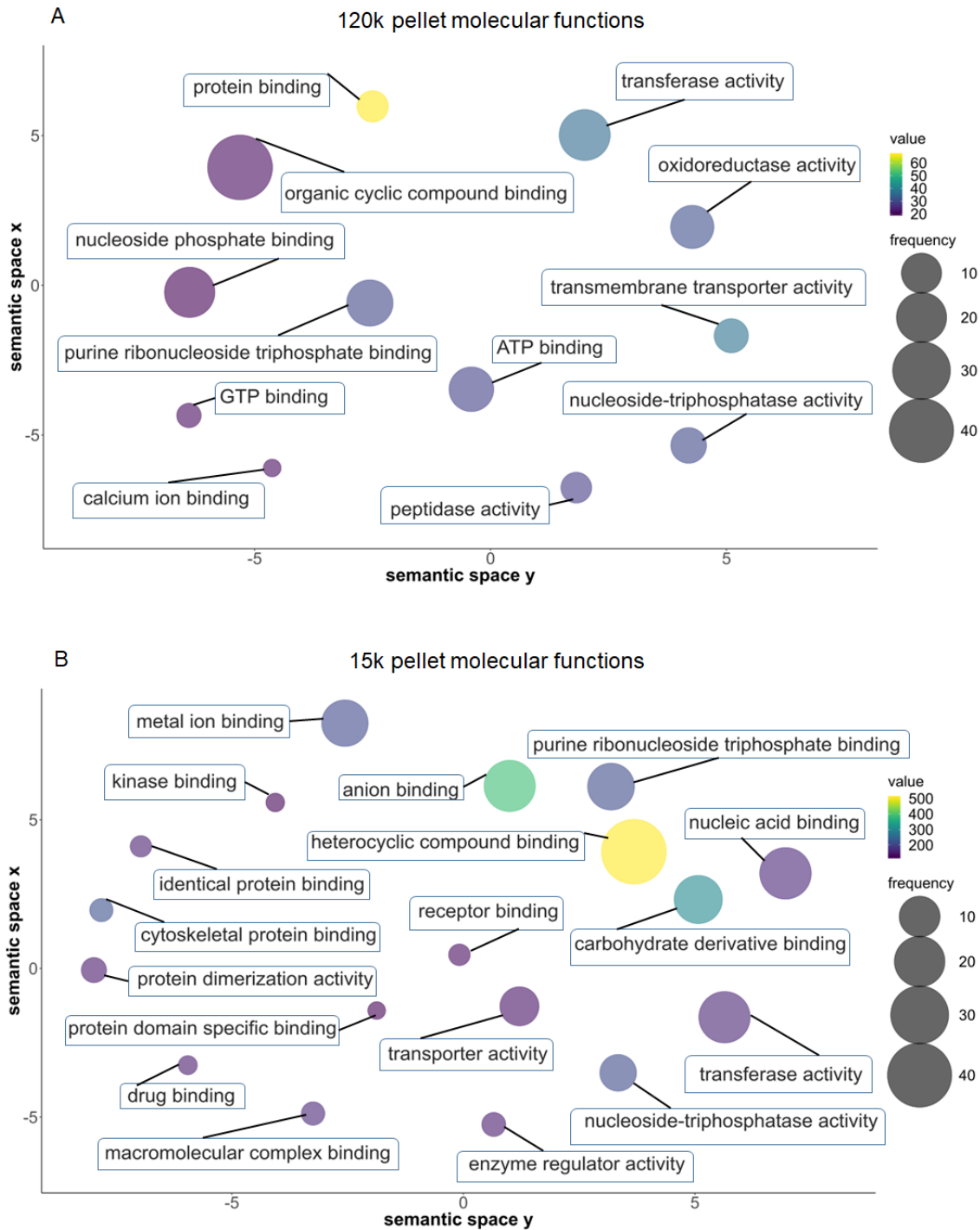
369 ***S. mansoni*-derived 120k (A) and 15k vesicles (B).** REViGO plot showing the most

370 abundantly represented GO terms ranked by nodescore (Blast2GO). Increasing heatmap

371 score signifies increasing nodescore from Blast2GO, while circle size denotes the

372 frequency of the GO term from the underlying database.

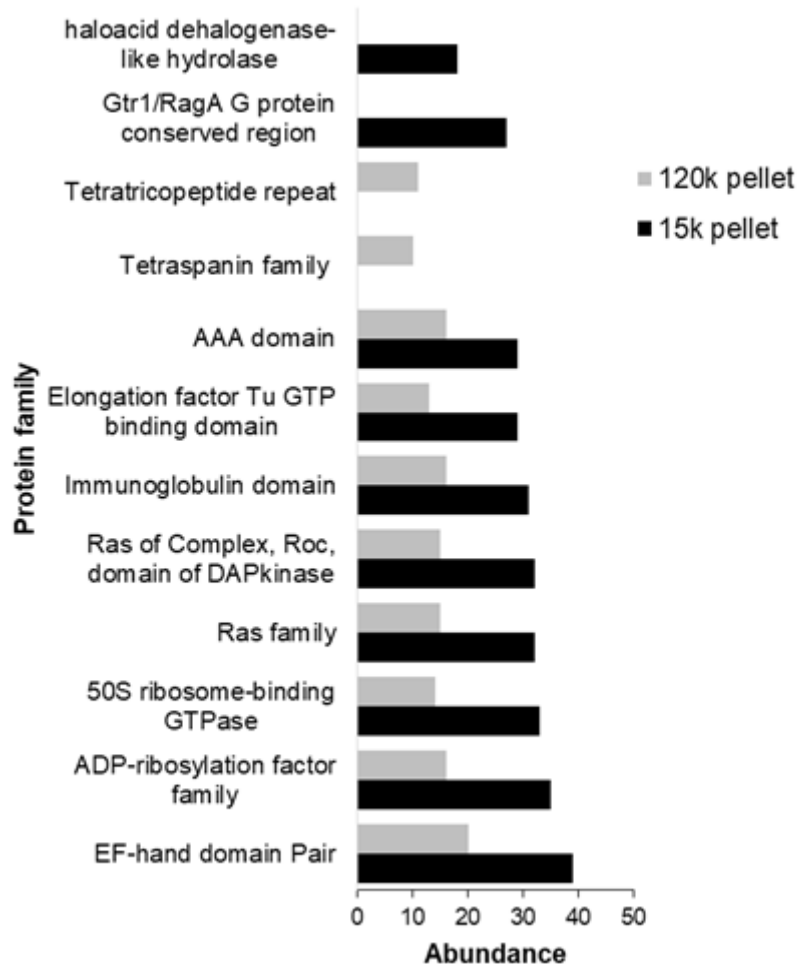
373



374

375 **Figure 6. Bioinformatic analysis of gene ontology molecular function terms in**
 376 **adult *S. mansoni*-derived 120k (A) and 15k vesicles (B).** REViGO plot showing the
 377 most abundantly represented GO terms ranked by nodescore (Blast2GO). Increasing
 378 heatmap score signifies increasing nodescore from Blast2GO, while circle size denotes
 379 the frequency of the GO term from the underlying database.

380 We have also reported the top 10 represented protein families in each vesicle type
 381 analysed (Figure 7). The eight most highly represented protein family domains (by
 382 amount of protein containing a particular domain) were common to both 120k and 15k
 383 pellet vesicles but presented different levels of abundance, including “EF-hand domain
 384 pair”, “ADP-ribosylation factor family”, “50s ribosome-binding GTPase” and “Ras”
 385 family proteins. In addition, proteins from the TSP family were abundant in the 120k
 386 vesicles but less well represented in the 15k vesicles. Protein families identified in both
 387 vesicle types analysed are presented in Supplementary Table S9 and Supplementary
 388 Table S10, respectively.



389

390 **Figure 7. Pfam analysis of the proteins secreted by *S. mansoni*-derived EVs.** Bar
391 graph showing the top 10 most represented protein families of 120k and 15k pellet
392 vesicles of adult *S. mansoni*.

393 From the total of 286 proteins identified in 120k pellet vesicles and 716 proteins
394 identified in 15k pellet vesicles, 39 (13.6%) and 64 (8.9 %) contained a signal peptide,
395 respectively (Supplementary Table S11 and 12), whereas 69 (24.1%) and 120 (16.8%)
396 of the proteins identified in 120k pellet (Supplementary Table S13) and 15k pellet
397 vesicles (Supplementary Table S14), respectively, contained transmembrane domains.

398 Functional annotation revealed proteins of potential relevance for host-parasite
399 communication in both types of EVs analysed, including proteases, protease inhibitors
400 and antioxidants in all compartments of EVs and proteins associated with membrane
401 structures from 120k pellet (Table 1) and 15k pellet (Table 2). Moreover, previously
402 described vaccine candidates, including, TSP-2, GST, Sm29, and calpain were
403 identified in both vesicle types, while the TSP Sm23 was identified only in 15k Pellet.
404 Moreover, proteases corresponding to cathepsin family proteins such as cathepsin B-
405 and cathepsin L-like proteases were identified in both EV types analysed. Other
406 proteases, including putative aminopeptidase W07G4.4, were released following trypsin
407 shaving of both EV types. In addition, proteins from the annexin group, including
408 annexin A3, annexin A7, annexin A8 and annexin A8-like protein 1, were identified
409 only in MVs. Protease inhibitors such as serpin B9 and cystatin-B were also identified
410 only in 15k pellet, while cysteine protease inhibitors were identified only in 120k pellet.
411 Further, proteins with antioxidant or defence roles such as thioredoxin peroxidase were
412 identified in both EV types analysed, whereas, peroxiredoxin Prx3 was only found in
413 120k pellet, and prostamide/prostaglandin F, thioredoxin peroxidase-2 and thioredoxin-
414 2 were anti-oxidant proteins found only in 15k pellet (Table 1 and 2).

415 We identified proteins involved in vesicle biogenesis and trafficking exclusively in
416 120k pellet vesicles including chmp1 (chromatin modified protein), charged MVB
417 proteins, vacuolar protein sorting-associated protein as well as Rab related proteins such
418 as Rab-2A, Rab-7a, Rab-27A and Ral A. Moreover, other vesicle biogenesis proteins
419 such as Ras related proteins (Rab-2B, Rab 6, Rab-10, Rab-14 and Rab-18) were
420 identified only in 15k pellet. In addition, proteins with similar roles such as charged
421 MVB protein 4b (SNF7 homolog associated with Alix 1), syntenin-1, annexin, Rab-8A
422 and Rab-11A were identified from both vesicles types. Further, common exosome
423 markers, such as heat shock protein (Hsp)-70, members of the TSP family (*Sm*TSP-1,
424 *Sm*-TSP-2, *Sm*-TSP-4 and putative TSP-18), Rab protein families and enolase were
425 identified in both EV types, and hsp-90 was identified only in 15k vesicles
426 (Supplementary Tables S1-8).

427 Membrane transporters, channels, and other molecules involved in membrane structure
428 were identified from different compartments of both EV types analysed including
429 aquaporin, Na⁺/K⁺-transporting ATPase, H⁺-transporting ATPase and phospholipid-
430 transporting ATPase IIB. Moreover, other proteins with potential roles in membrane
431 structure and signalling including, the TSPs noted above, as well as Sm13 and the 25
432 kDa integral membrane protein, were identified in both vesicle types, whereas other
433 membrane proteins were unique to just one vesicle population, including the 200 kDa
434 GPI-anchored surface glycoprotein, found in 120k pellet only, and Sm23, tegument
435 antigen (I(H)A) and CD 151 homologue, found in 15k pellet vesicles only (Tables 1 and
436 2 and Supplementary Tables S1-8).

437

438

440 **Table 2.** Functional annotations of proteins from adult *Schistosoma mansoni*-derived 15k
 441 pellet vesicles.

| Accession number | Description | # unique peptides | | | |
|------------------|--|-------------------|-------|------|------|
| | | TLPs | Cargo | IMPs | PMPs |
| Smp_089670.1 | Alpha-2-macroglobulin-like protein 1 | 2 | 11 | 3 | 2 |
| Smp_089180.1 | Ubiquitin carboxyl-terminal hydrolase 7 | 2 | 0 | 3 | 0 |
| Smp_100090.1 | High mobility group protein DSP1 | 2 | 0 | 0 | 0 |
| Smp_103610.1 | Cathepsin B-like peptidase (C01 family) | 2 | 0 | 6 | 2 |
| Smp_187140.1 | Cathepsin L-like proteinase precursor | 4 | 2 | 5 | 3 |
| Smp_207080.1 | Proteasome subunit alpha type-6 | 5 | 2 | 0 | 0 |
| Smp_214190.1 | Calpain | 6 | 12 | 41 | 4 |
| Smp_153960.1 | Presenilin homolog | 3 | 0 | 0 | 0 |
| Smp_155720.1 | Glycogen synthase kinase-3 alpha | 3 | 0 | 0 | 0 |
| Smp_141610.1 | Cathepsin B-like cysteine proteinase | 3 | 2 | 3 | 0 |
| Smp_212880.1 | Proteasome subunit beta type-5 | 5 | 0 | 0 | 0 |
| Smp_172590.1 | family S10 unassigned peptidase (S10 family) | 4 | 4 | 10 | 3 |
| Smp_247170.1 | Major egg antigen | 6 | 0 | 3 | 0 |
| Smp_340060.1 | Mastin precursor | 13 | 13 | 17 | 9 |
| Smp_343260.1 | cathepsin L, a | 23 | 0 | 12 | 12 |
| Smp_346350.1 | 26S proteasome non-ATPase regulatory subunit 1 | 38 | 0 | 2 | 0 |
| Smp_246110.1 | Kyphoscoliosis peptidase | 6 | 0 | 7 | 4 |
| Smp_307450.1 | U-actitoxin-Avd3s | 8 | 0 | 0 | 0 |
| Smp_303330.1 | Hemoglobinase | 7 | 0 | 0 | 0 |
| Smp_032580.1 | Proteasome subunit alpha type-5 | 0 | 3 | 2 | 0 |
| Smp_013040.1 | Lysosomal aspartic protease | 0 | 2 | 6 | 0 |
| Smp_074500.1 | Proteasome subunit beta type-2 | 0 | 2 | 0 | 0 |
| Smp_070930.1 | Proteasome subunit alpha type-4 | 0 | 3 | 3 | 0 |
| Smp_071610.1 | Dipeptidyl peptidase 2 | 0 | 2 | 4 | 0 |
| Smp_034490.1 | Proteasome subunit beta type-6 | 0 | 5 | 4 | 0 |
| Smp_082030.1 | Protein dj-1beta | 0 | 3 | 3 | 0 |
| Smp_092280.1 | 20S proteasome subunit alpha 7 | 0 | 3 | 2 | 2 |
| Smp_076230.1 | Proteasome subunit alpha-type 7-like | 0 | 2 | 0 | 0 |
| Smp_212920.1 | Proteasome subunit alpha type-1 | 0 | 4 | 0 | 0 |
| Smp_301340.1 | Proteasome subunit beta type-1-B | 0 | 4 | 0 | 0 |
| Smp_006390.1 | Cystatin-B | 0 | 0 | 6 | 0 |
| Smp_008545.1 | 60 kDa heat shock protein, mitochondrial | 0 | 0 | 3 | 0 |
| Smp_027610.1 | 40S ribosomal protein S3 | 0 | 0 | 3 | 0 |
| Smp_022400.1 | Glucose-6-phosphate isomerase | 0 | 0 | 11 | 0 |
| Smp_030000.1 | Putative aminopeptidase W07G4.4 | 0 | 0 | 21 | 0 |
| Smp_028500.1 | Caspase-3 | 0 | 0 | 2 | 0 |
| Smp_018240.1 | Transitional endoplasmic reticulum ATPase | 0 | 0 | 19 | 0 |
| Smp_019010.1 | Dipeptidyl peptidase 3 | 0 | 0 | 9 | 0 |

| | | | | | |
|--------------|---|---|---|----|---|
| Smp_029500.1 | Thimet oligopeptidase | 0 | 0 | 4 | 0 |
| Smp_061920.1 | UV excision repair protein RAD23 homolog B | 0 | 0 | 5 | 0 |
| Smp_056970.2 | Glyceraldehyde-3-phosphate dehydrogenase | 0 | 0 | 27 | 0 |
| Smp_031730.1 | Signal peptidase complex catalytic subunit SEC11C | 0 | 0 | 2 | 0 |
| Smp_067490.1 | Sorcin | 0 | 0 | 6 | 0 |
| Smp_067480.1 | Sorcin | 0 | 0 | 6 | 0 |
| Smp_033710.1 | ATP-dependent RNA helicase DDX3Y | 0 | 0 | 3 | 0 |
| Smp_067060.1 | Cathepsin B-like cysteine proteinase | 0 | 0 | 5 | 0 |
| Smp_089460.1 | Calpain-B | 0 | 0 | 13 | 0 |
| Smp_083870.1 | Putative aminopeptidase W07G4.4 | 0 | 0 | 5 | 0 |
| Smp_099030.1 | Casein kinase II subunit alpha | 0 | 0 | 5 | 0 |
| Smp_136640.1 | Sorcin | 0 | 0 | 5 | 0 |
| Smp_085640.1 | COP9 signalosome complex subunit 4 | 0 | 0 | 2 | 0 |
| Smp_079770.1 | Probable protein disulfide-isomerase ER-60 | 0 | 0 | 2 | 0 |
| Smp_090800.1 | Xaa-Pro dipeptidase | 0 | 0 | 3 | 0 |
| Smp_102040.1 | Guanine nucleotide-binding protein subunit beta-2-like 1 | 0 | 0 | 3 | 0 |
| Smp_072140.1 | Rho-related GTP-binding protein RhoC | 0 | 0 | 5 | 0 |
| Smp_091470.1 | Puromycin-sensitive aminopeptidase | 0 | 0 | 4 | 0 |
| Smp_104110.1 | Ras-like GTP-binding protein RHO | 0 | 0 | 4 | 0 |
| Smp_089100.1 | Glutathione hydrolase 7 | 0 | 0 | 12 | 0 |
| Smp_075800.1 | Hemoglobinase | 0 | 0 | 7 | 0 |
| Smp_247080.1 | Aminopeptidase N | 0 | 0 | 3 | 4 |
| Smp_165490.1 | Serine/threonine-protein phosphatase 2A catalytic subunit alpha isoform | 0 | 0 | 3 | 0 |
| Smp_155560.1 | Serpin B9 | 0 | 0 | 2 | 0 |
| Smp_213550.1 | 26S proteasome non-ATPase regulatory subunit 14 | 0 | 0 | 2 | 0 |
| Smp_213240.1 | Prolyl endopeptidase | 0 | 0 | 7 | 0 |
| Smp_243200.1 | Calpain-7 | 0 | 0 | 2 | 0 |

Biogenesis/vesicle trafficking

| | | | | | |
|--------------|---|----|---|----|---|
| Smp_099310.1 | Protein transport protein Sec23A | 2 | 0 | 3 | 0 |
| Smp_118830.1 | F-actin-capping protein subunit alpha-2 | 2 | 0 | 3 | 0 |
| Smp_131870.2 | Syntaxin-binding protein 1 | 3 | 0 | 0 | 0 |
| Smp_157410.1 | Cytoplasmic dynein 1 heavy chain 1 | 3 | 0 | 0 | 0 |
| Smp_154420.1 | clathrin heavy chain | 3 | 0 | 14 | 3 |
| Smp_332400.1 | Coatomer subunit delta | 12 | 0 | 3 | 0 |
| Smp_333910.1 | F-actin-capping protein subunit beta | 12 | 0 | 5 | 0 |
| Smp_008660.2 | Severin | 0 | 0 | 7 | 0 |
| Smp_071630.1 | Ras-related protein Rab-2B | 0 | 0 | 11 | 0 |
| Smp_077720.2 | Annexin A5 | 0 | 0 | 4 | 0 |
| Smp_004910.1 | Ras-related protein Rab-14 | 0 | 0 | 4 | 0 |
| Smp_005670.1 | Ras-related protein Rab-11A | 0 | 0 | 2 | 0 |
| Smp_014020.1 | Cell cycle control protein 50A | 0 | 0 | 3 | 0 |
| Smp_010090.1 | Charged multivesicular body protein 5 | 0 | 0 | 3 | 0 |
| Smp_008230.1 | Ras-related protein Rab-18 | 0 | 0 | 4 | 0 |

| | | | | | |
|--------------|---|---|---|----|---|
| Smp_014660.1 | Ras-related protein Rab-10 | 0 | 0 | 4 | 0 |
| Smp_048940.1 | Vacuolar protein sorting-associated protein 37B | 0 | 0 | 2 | 0 |
| Smp_045710.1 | Charged multivesicular body protein 4b | 0 | 0 | 6 | 0 |
| Smp_055880.1 | Charged multivesicular body protein 1a | 0 | 0 | 8 | 0 |
| Smp_032150.1 | Charged multivesicular body protein 3 | 0 | 0 | 3 | 0 |
| Smp_047450.1 | Synaptobrevin homolog YKT6 | 0 | 0 | 3 | 0 |
| Smp_057320.1 | Vesicle-fusing ATPase 2 | 0 | 0 | 4 | 0 |
| Smp_035620.1 | Multivesicular body subunit 12B | 0 | 0 | 2 | 0 |
| Smp_045500.1 | Annexin A7 | 0 | 0 | 4 | 0 |
| Smp_034870.1 | AP-2 complex subunit beta | 0 | 0 | 5 | 0 |
| Smp_055870.1 | Vesicle-associated membrane protein 8 | 0 | 0 | 7 | 0 |
| Smp_104670.1 | Ras-related protein Rab-8A | 0 | 0 | 4 | 0 |
| Smp_146400.1 | Syntaxin-binding protein 1 | 0 | 0 | 3 | 0 |
| Smp_074020.1 | AP-2 complex subunit alpha | 0 | 0 | 6 | 0 |
| Smp_093230.1 | Actin-related protein 10 | 0 | 0 | 2 | 0 |
| Smp_068530.1 | Syntenin-1 | 0 | 0 | 10 | 0 |
| Smp_092770.1 | Coatomer subunit gamma-2 | 0 | 0 | 2 | 0 |
| Smp_079000.1 | Charged multivesicular body protein 1b | 0 | 0 | 3 | 0 |
| Smp_104310.1 | Ras-related protein Rab-11A | 0 | 0 | 5 | 0 |
| Smp_174580.1 | Vesicular integral-membrane protein VIP36 | 0 | 0 | 2 | 0 |
| Smp_169460.1 | GTP-binding protein YPTC1 | 0 | 0 | 7 | 0 |
| Smp_210250.1 | Cell cycle control protein 50A | 0 | 0 | 8 | 0 |
| Smp_340230.1 | Charged multivesicular body protein 2a | 0 | 0 | 4 | 0 |
| Smp_245450.1 | Coatomer subunit alpha | 0 | 0 | 3 | 0 |
| Smp_337410.1 | Tumor susceptibility gene 101 protein | 0 | 0 | 3 | 0 |
| Smp_163580.1 | Ras-related protein Rab6 | 0 | 0 | 2 | 0 |

Antioxidants

| | | | | | |
|--------------|-------------------------------------|---|---|---|---|
| Smp_194940.1 | Prostamide/prostaglandin F synthase | 4 | 0 | 7 | 0 |
| Smp_158110.1 | Thioredoxin peroxidase | 3 | 3 | 7 | 3 |
| Smp_309480.1 | Thioredoxin peroxidase 2 | 8 | 6 | 9 | 5 |
| Smp_008070.1 | Thioredoxin-2 | 0 | 3 | 2 | 0 |

Membrane structure

| | | | | | |
|--------------|--|----|---|----|----|
| Smp_121160.2 | Mitochondrial dicarboxylate carrier | 2 | 0 | 0 | 0 |
| Smp_103200.1 | V-type proton ATPase subunit D | 2 | 0 | 8 | 0 |
| Smp_099890.1 | Receptor expression-enhancing protein 5 | 2 | 2 | 5 | 2 |
| Smp_104270.1 | Bis(5'-adenosyl)-triphosphatase enpp4 | 2 | 0 | 20 | 2 |
| Smp_127820.1 | SJCHGC05417 protein | 2 | 0 | 0 | 2 |
| Smp_130300.1 | Sodium/potassium-transporting ATPase subunit alpha | 3 | 0 | 12 | 0 |
| Smp_130280.1 | cell polarity protein | 3 | 0 | 0 | 2 |
| Smp_141010.1 | Dysferlin | 3 | 0 | 0 | 2 |
| Smp_340630.1 | putative endoplasmic | 15 | 0 | 0 | 10 |
| Smp_313560.1 | alkaline phosphatase | 9 | 4 | 17 | 6 |
| Smp_315900.1 | Plasma membrane calcium-transporting ATPase 3 | 10 | 0 | 2 | 0 |
| Smp_005720.1 | Aquaporin-3 | 0 | 2 | 5 | 0 |

| | | | | | |
|--------------|---|---|---|----|---|
| Smp_020370.1 | Reticulon-4 | 0 | 2 | 7 | 0 |
| Smp_017430.1 | 23 kDa integral membrane protein | 0 | 4 | 16 | 0 |
| Smp_012440.1 | Solute carrier family 2, facilitated glucose transporter member 1 | 0 | 7 | 13 | 0 |
| Smp_041460.1 | tetraspanin D76 | 0 | 2 | 8 | 0 |
| Smp_153390.1 | putative ectonucleotide pyrophosphatase/phosphodiesterase | 0 | 7 | 5 | 3 |
| Smp_155310.1 | tetraspanin, putative (<i>Sm-TSP-1</i>) | 0 | 2 | 6 | 0 |
| Smp_140000.1 | putative tetraspanin-CD63 receptor (<i>Sm-TSP-4</i>) | 0 | 5 | 8 | 2 |
| Smp_162770.1 | lysosome-associated membrane glycoprotein | 0 | 2 | 0 | 3 |
| Smp_335630.1 | tetraspanin 2 (<i>Sm-TSP-2</i>) | 0 | 6 | 7 | 8 |
| Smp_300190.1 | Aquaporin-9 (AQP-9) (Small solute channel 1) | 0 | 3 | 6 | 4 |
| Smp_267000.1 | ATPase, H ⁺ transporting, lysosomal accessory protein 1 | 0 | 2 | 7 | 4 |
| Smp_007260.1 | Sarcoplasmic/endoplasmic reticulum calcium ATPase 2 | 0 | 0 | 3 | 0 |
| Smp_011560.1 | CD151 antigen | 0 | 0 | 5 | 0 |
| Smp_029390.1 | V-type proton ATPase subunit B | 0 | 0 | 14 | 0 |
| Smp_015020.1 | Sodium/potassium-transporting ATPase subunit alpha | 0 | 0 | 22 | 0 |
| Smp_024820.1 | CD9 antigen | 0 | 0 | 3 | 0 |
| Smp_048230.1 | High affinity copper uptake protein 1 | 0 | 0 | 4 | 0 |
| Smp_039130.1 | NPC intracellular cholesterol transporter 1 | 0 | 0 | 16 | 0 |
| Smp_055780.1 | Multidrug resistance protein 1 | 0 | 0 | 54 | 0 |
| Smp_040080.1 | Glycosylated lysosomal membrane protein B | 0 | 0 | 7 | 0 |
| Smp_059530.1 | 25 kDa integral membrane protein | 0 | 0 | 3 | 0 |
| Smp_091650.1 | putative phospholipid-transporting ATPase IIB | 0 | 0 | 20 | 2 |
| Smp_136710.1 | putative calcium-transporting atpase sarcoplasmic/endoplasmic reticulum type (calcium pump) | 0 | 0 | 7 | 2 |
| Smp_105680.1 | Dolichyl-diphosphooligosaccharide--protein glycosyltransferase subunit 1 | 0 | 0 | 2 | 0 |
| Smp_105410.1 | Solute carrier family 2, facilitated glucose transporter member 3 | 0 | 0 | 4 | 0 |
| Smp_129820.1 | Canalicular multispecific organic anion transporter 2 | 0 | 0 | 9 | 0 |
| Smp_131890.1 | Sodium- and chloride-dependent glycine transporter 1 | 0 | 0 | 2 | 0 |
| Smp_127940.1 | Sodium-driven chloride bicarbonate exchanger | 0 | 0 | 2 | 0 |
| Smp_123280.1 | Major facilitator superfamily domain-containing protein 1 | 0 | 0 | 15 | 0 |
| Smp_130230.1 | Ras-related protein Rac1 | 0 | 0 | 2 | 0 |
| Smp_128940.1 | Metabotropic glutamate receptor 7 | 0 | 0 | 3 | 0 |
| Smp_136240.1 | Vesicle-associated membrane protein/synaptobrevin-binding protein | 0 | 0 | 3 | 0 |
| Smp_141680.1 | Fasciclin-1 | 0 | 0 | 2 | 0 |

| | | | | | |
|--------------|---|---|---|----|----|
| Smp_079220.1 | ADP,ATP carrier protein | 0 | 0 | 3 | 0 |
| Smp_082810.1 | Cell division control protein 42 homolog | 0 | 0 | 7 | 0 |
| Smp_069120.1 | Synaptotagmin-2 | 0 | 0 | 11 | 0 |
| Smp_075210.1 | Prohibitin-2 | 0 | 0 | 3 | 0 |
| Smp_127650.1 | Secretory carrier-associated membrane protein 1 | 0 | 0 | 2 | 0 |
| Smp_099150.1 | Pleckstrin homology domain-containing family B member 2 | 0 | 0 | 4 | 0 |
| Smp_162510.1 | Solute carrier family 46 member 3 | 0 | 0 | 5 | 0 |
| Smp_246400.1 | Glycosyltransferase 1 domain-containing protein 1 | 0 | 0 | 6 | 4 |
| Smp_173150.1 | CD63 antigen | 0 | 0 | 2 | 0 |
| Smp_167240.1 | Nicastrin | 0 | 0 | 3 | 0 |
| Smp_332300.1 | Glucose-6-phosphate exchanger SLC37A2 | 0 | 0 | 2 | 0 |
| Smp_194920.1 | T-cell immunomodulatory protein | 0 | 0 | 12 | 3 |
| Smp_246270.1 | ATP-binding cassette sub-family B member 6, mitochondrial | 0 | 0 | 16 | 4 |
| Smp_196110.1 | Ferric-chelate reductase 1 | 0 | 0 | 6 | 0 |
| Smp_176940.1 | High affinity cationic amino acid transporter 1 | 0 | 0 | 4 | 0 |
| Smp_333250.1 | Putative phospholipid-transporting ATPase C4F10.16c | 0 | 0 | 3 | 0 |
| Smp_171870.1 | Synaptic vesicle 2-related protein; Short=SV2-related protein | 0 | 0 | 3 | 0 |
| Smp_244710.1 | ATP-binding cassette sub-family A member 3 | 0 | 0 | 2 | 0 |
| Smp_344440.1 | putative tetraspanin 18, isoform 1 | 0 | 0 | 6 | 14 |
| Smp_343120.1 | Plasma membrane calcium-transporting ATPase 3 | 0 | 0 | 13 | 0 |
| Smp_160160.1 | Sialin | 0 | 0 | 2 | 0 |
| Smp_340540.1 | lysosome membrane protein 2 | 0 | 0 | 6 | 9 |
| Smp_245370.1 | Equilibrative nucleoside transporter 3 | 0 | 0 | 3 | 0 |
| Smp_190770.1 | LanC-like protein 2 | 0 | 0 | 0 | 3 |
| Smp_248070.1 | putative dock | 0 | 0 | 0 | 4 |
| Smp_315840.1 | Kinase D-interacting substrate of 220 kDa | 0 | 0 | 0 | 6 |
| Smp_336620.1 | Gamma-aminobutyric acid receptor subunit gamma-3 | 0 | 0 | 0 | 9 |
| Smp_323680.1 | SJCHGC06792 protein | 0 | 0 | 0 | 8 |
| Smp_095630.1 | CD81 antigen | 0 | 0 | 3 | 0 |

442

443

444 **4. Discussion**

445 Cells release different populations of EVs, which may either derive from the endosomal

446 pathway, formed by inward budding of the MVB membrane and allowing capture of

447 cytoplasmic cargo (exosomes, 30-150 nm in diameter), or bud directly from their plasma
448 membrane (MVs, 100-1000 nm in diameter) (36). In this work, a proteomic analysis of two
449 subpopulations of EVs secreted from adult *S. mansoni* was performed to gain more
450 comprehensive coverage of these EV proteomes. The 120k pellet vesicles that we isolated
451 fit the characteristics and flotation properties on a iodixanol-density gradient for
452 classification as exosomes (37). Moreover, the size distribution and concentration of both
453 *S. mansoni*-derived 120k and 15k pellet vesicles were analysed by TRPS, allowing us to
454 confirm the presence of these EV types. Importantly, well-standardized techniques (38)
455 were used to isolate these two EV types, giving us confidence in the purity of our vesicle
456 samples.

457

458 The 120k pellet sample purified in the present study had a higher purity (number of
459 particles/ μ g of protein) than the 15k pellet sample. The purity ratio was primarily
460 described for exosomes (26), but, in general, since MVs are physically larger than
461 exosomes, it is expected that they contain more proteins and hence the purity ratio should
462 be lower. However, our results do not show significant differences in size between both
463 types of samples, and we might speculate that the differences in protein composition might
464 be due to the different release pathways followed by both EV types. Despite our results
465 agreeing with previous studies (14, 26), it is worth noting that purity should be estimated
466 for each organism or type of sample analysed. The particle diameter range for the two
467 vesicle types appeared to be similar and overlapped (39). Accordingly, the size range of
468 120k vesicles had a wider range than that of 15k vesicles, however the mean size obtained
469 corresponded to that of exosomes (19). 15k vesicles, however, had a relatively higher
470 concentration (particles/ml) than 120k vesicles for any given size (Figure 2A and 2B).
471 Although apoptotic bodies differ clearly from exosomes by their larger size, other vesicle

472 types are more difficult to separate since MVs with a similar size to exosomes can also bud
473 at the plasma membrane (40). Moreover, the size overlap observed between the two
474 vesicles analysed can be explained at least in part by the nanopore size used to measure the
475 size distribution of these vesicles – NP150 was used to analyse 120k pellet (60 to 480 nm)
476 whereas NP300 was used for 15k pellet vesicles (115 to 1150 nm). Several studies have
477 reported helminth EVs that correspond to exosomes in terms of vesicle size, including *S.*
478 *mansoni* (14, 15, 41), other trematodes (17, 42-45), nematodes (21, 34, 35, 46-51), and
479 cestodes (52-54). To our knowledge, only one study was done prior to ours involved
480 helminth-derived MVs which reported a 15k pelleted fraction from *F. hepatica* (44) with
481 size range of 50-200nm and, furthermore, 15k pellet vesicles analysed in this study were
482 within the expected size range for mammalian MVs (19). Using sequential extraction to
483 attribute proteins to sub-vesicular compartments of EVs coupled with highly accurate
484 tandem mass spectrometry, we identified more than twice as many 120k vesicles proteins
485 than reported earlier (14).

486

487 To determine the location of each protein within their respective vesicles, we performed a
488 sequential extraction as describe previously for *F. hepatica*- (44) and *Mycoplasma*
489 *hyopneumoniae*-derived exosomes (27). Proteins identified with high abundance following
490 trypsin shaving of both 120k and 15k pellet vesicles include a fatty acid binding protein
491 with a role in biosynthesis of fatty acids and cholesterol in schistosomes (55), the
492 antioxidants thioredoxin peroxidase (56) and GST (57, 58), dynein light chain (59) and
493 membrane structure proteins, for example the Sm13 tegument antigen (60). Proteases and
494 peptidases including calpain, cathepsins B, cathepsin L, cathepsin A, legumain, and a Pro-
495 Xaa carboxypeptidase were also identified following trypsin shaving of both vesicle types
496 analysed but with relatively less abundance. Similar peptidases were released following

497 trypsin shaving of the *F. hepatica*-derived EV surface (44). Whether these proteases and
498 peptidases, many of which do not contain transmembrane or other membrane-anchoring
499 motifs, are found on the surface of EVs *in vivo* remains to be determined. Proteases and
500 other enzymes have been reported on the surface of mammalian exosomes following
501 invagination of the cell membrane whereby molecules on the cell surface become localized
502 to the luminal side of the endosomal membrane. Some of these proteases then make their
503 way to the exosome surface through small invaginations of the endosomal membrane
504 where they remain once the multi-vesicular body forms and eventually fuses with the cell
505 membrane to release the newly formed exosome into the extracellular space (61). Another
506 possibility is that soluble proteases bind to the exosome surface within either the
507 endosomal compartment or following secretion of the exosomes into the extracellular
508 space. Once localized to the exosome surface, proteases are free to encounter substrates
509 either at the cell surface or within the extracellular matrix, including ectodomain shedding
510 (62). Interestingly, most of the proteases associated with the mammalian cell surface are
511 metalloproteases, particularly matrix metalloproteases (62), whereas there was only a
512 single MMP (nardilysin or ADAM17) identified on the 15k vesicles surface and none were
513 detected on 120k vesicles despite the presence of a family of leishmanolysin-like clan M
514 metalloproteases in the *S. mansoni* genome (63). Instead, cysteine proteases were
515 abundantly represented on the surface of the schistosome vesicles, reflecting their genome-
516 wide over-representation in many blood-feeding helminths (64), and suggestive of a role
517 for EVs in feeding.

518 HSP-70 (65, 66) and TSPs (38, 67) are widely considered as biomarkers of EVs from
519 mammalian cells; for example, HSP-70 has been reported from MVs (19, 68, 69) and the
520 TSPs CD9, CD63 and CD81 have been found in exosomes, MVs and apoptotic bodies (40,
521 70, 71). Similarly, our data support these findings in that HSP-70 was identified in both

522 120k pellet (identified in cargo and PMP compartments) and 15k pellet (TLP and PMP
523 compartments). Likewise, members of the TSP family including *Sm*-TSP-1, TSP-2, and
524 TSP-4 were identified in cargo, PMP and IMP compartments of both vesicle analysed. Our
525 data presented herein revealed that 15k and 120k vesicles share many proteins, notably the
526 surface membrane TSPs, so distinguishing EV types by their proteomic content requires
527 caution. While unique proteins were identified in both 120k and 15k pellet vesicles,
528 confirmation of the specificity of these markers to each vesicle population, by western
529 blotting or immunogold transmission electron microscopy, will be an important focus of
530 future studies. A recent study has identified annexin-1 and CD63 (a protein from the
531 tetraspanin family) as specific markers in MVs and exosomes, respectively, from human
532 cells (69). We have identified several annexins that are present only in the 15k pellet
533 vesicles; all tetraspanins identified were present in both populations. This highlights the
534 difficulty in obtaining specific markers for non-human and non-mammalian EVs and the
535 need to advance the field in this direction. Now that a catalogue of shared and unique EV
536 sub-type proteins has been produced, antibodies to select candidate proteins can be
537 generated to aid in classifying the various cellular/tissue origins of helminth EVs and to
538 monitor their trafficking and release.

539 Previously described schistosomiasis vaccine candidates were identified in both 120k and
540 15k vesicles, including TSP-2 (72), GST (73, 74), Sm29 (75) and calpain (76-78), whereas
541 Sm23 (73, 79) was identified from cargo and IMP components of 15k vesicles only.
542 Indeed, TSP-2, GST, and Sm29 were among the most abundant proteins identified in both
543 EV types, further supporting the notion of EVs as a major reservoir of vaccine candidates
544 against schistosomiasis and other helminth infections. Our data also showed clear abundant
545 of schistosome surface antigens such as TSP-1, TSP-2, TSP-4, as well as TSP-18
546 (relatively with less abundance) and a variety of other tegumental antigens in both EV

547 types analysed, some of which have been implicated in schistosome evasion of the host
548 immune response (80, 81). Although TSP-1 has been reported to have vaccine efficacy in a
549 mouse model (72), TSP-4 and TSP-18 remain to be tested. EVs secreted by other related
550 trematodes were also found to be abundant in TSPs (44, 82). Further, antibodies generated
551 against an EV surface TSP were able to block the internalization of *O. viverrini* EVs by
552 human cholangiocytes (45), and EVs and recombinant TSPs from *O. viverrini* and other
553 helminth parasites have been shown to be efficacious as vaccines in animal models (22, 23,
554 51).

555 One of the proteins identified from the integral membrane component of both vesicle types
556 was annexin, a protein involved in a wide range of cellular processes, and, notably has an
557 anti-inflammatory role (83). Moreover, annexins function as plasminogen receptors and
558 enhance fibrinolysis-prolonging blood clot formation (84), roles that are likely to be
559 important for an intra-vascular parasite. Together with the identification of other proteins
560 with known and proposed roles in red cell lysis (saponin-like proteins) (85), haem storage
561 (ferritin isoforms) and blood feeding (endoproteases and aminopeptidases), a role is
562 emerging for EVs in the nutrient acquisition process in haematophagous trematode
563 parasites. Moreover, enolase, found in both EV types in this study, has been identified as a
564 tissue plasminogen activator which subsequently results in the generation of the potent
565 fibrinolytic agent plasmin which could degrade blood clots forming around *S. mansoni*
566 parasites *in vivo* (86).

567 Proteins involved in vesicle biogenesis and trafficking were particularly abundant in the
568 IMP compartment of both vesicle types. Among these were members of the endosomal
569 sorting complex required for transport-I and -III pathways with known essential roles in
570 vesicle biogenesis and secretion in mammalian cells (87). Charged MVB proteins such as

571 chromatin modified protein (chmp1) were identified only in 120k pellet. It was unexpected
572 to identify proteins involved in exosome biogenesis also in 15k vesicles. While every
573 effort was made to minimise the occurrence of contamination of 15k sample by 120k
574 pellet, we could not discount the possibility of isolation of 120k vesicles (if at all) in 15k
575 pellet sample preparation. Moreover, while maximum effort was dedicated to keeping our
576 ES, and hence EV samples, free of any egg-secreted molecules, the possibility of minor
577 contamination with egg secretions cannot be wholly discounted. Even though the
578 generation of MVs and exosomes occurs at distinct sites within the cell, common
579 intracellular mechanisms and sorting machineries are involved in the biogenesis of both
580 entities (reviewed in (19)). In many cases, these shared mechanisms hinder the possibility
581 of distinguishing between the different vesicle sub-populations (20). Further, Rab
582 GTPases/Ras family proteins (identified in IMP and PMPs) such as Rab-2A, Rab-7a, Rab-
583 27A and Ral-A identified only in 120k pellet and Rab-2B, Rab 6, Rab-10, Rab-14 and
584 Rab-18 in 15k pellet were identified, while Rab-8A as well as Rab-11A were identified
585 from both vesicle types analysed. Ral-A is a small GTPase required for MVB biogenesis
586 and EV release in *Caenorhabditis elegans* (88) and *F. hepatica* (89). In contrary to our
587 findings, Rab10 has been detected in *S. japonicum*- (17) and *F. hepatica*-derived exosomes
588 (89). It was unexpected to identify Rab proteins, usually involved in 120k vesicle
589 biogenesis and trafficking (90), also in 15k samples, but this might be explained by the
590 reasons mentioned earlier. Rab proteins are one of the main regulators of intracellular EV
591 trafficking between subcellular compartments through processes including vesicle
592 budding, mobility along the cytoskeleton, and membrane fusion (91).

593

594 **5. Conclusions**

595 Herein, we have isolated and characterised the proteomic composition of two sub-
596 populations of *S. mansoni*-secreted EVs (120k and 15k pellet vesicles) using sequential
597 extraction of proteins from the different sub-vesicular compartments to provide a
598 comprehensive molecular snapshot. Future research should investigate whether *S. mansoni*
599 EVs interact with defined host cell types as it is unclear whether they are internalised by
600 host cells. A more comprehensive understanding of schistosome EV biology will facilitate
601 development of methods to interrupt vesicle-mediated communication between host and
602 parasite, as well as inter-parasite interactions. Schistosome EVs are clearly a rich source of
603 target antigens for the development of novel approaches for preventing, treating and
604 diagnosing infections, and we hope that further research continues to add to the
605 schistosomiasis control toolbox.

606

607 **Acknowledgements**

608 We thank Atik Susianto for maintenance of experimental mice and snails. We also thank
609 the Biomedical Research Institute, Rockville, MD, USA, especially Dr. Margaret Mentink-
610 Kane for provision of infected snails. This work was supported by a program grant from
611 the National Health and Medical Research Council (NHMRC, APP1132975) and a Senior
612 Principal Research fellowship from NHMRC to AL (APP1117504). DWK was supported
613 by an International Postgraduate Research Scholarship from James Cook University. The
614 funders had no role in the study design, data collection and analysis, decision to publish or
615 preparation of the manuscript. The authors declare no competing financial interests.

616

617 **References**

618 1. Mutapi F, Maizels R, Fenwick A, Woolhouse M. Human schistosomiasis in the post mass
619 drug administration era. *Lancet Infect Dis.* 2017;17(2):e42-e8.

- 620 2. McManus DP, Dunne DW, Sacko M, Utzinger J, Vennervald BJ, Zhou X-N.
621 Schistosomiasis. Nat Rev Dis Primers 2018;4(1):13.
- 622 3. Gryseels B, Polman K, Clerinx J, Kestens L. Human schistosomiasis. The Lancet.
623 2006;368(9541):1106-18.
- 624 4. Collins JJ, Wang B, Lambrus BG, Tharp ME, Iyer H, Newmark PA. Adult somatic stem
625 cells in the human parasite *Schistosoma mansoni*. Nature. 2013;494(7438):476-9.
- 626 5. Wang W, Liang Y. Mass drug administration (MDA) for schistosomiasis. J Infect Dis.
627 2015;211(5):848-9.
- 628 6. Knudsen GM, Medzihradzky KF, Lim K-C, Hansell E, McKerrow JH. Proteomic analysis
629 of *Schistosoma mansoni* cercarial secretions. Mol Cell Proteomics. 2005;4(12):1862-75.
- 630 7. Liu F, Cui SJ, Hu W, Feng Z, Wang ZQ, Han ZG. Excretory/secretory proteome of the
631 adult developmental stage of human blood fluke, *Schistosoma japonicum*. Mol Cell Proteomics.
632 2009;8(6):1236-51.
- 633 8. Perez-Sanchez R, Ramajo-Hernandez A, Ramajo-Martin V, Oleaga A. Proteomic analysis
634 of the tegument and excretory-secretory products of adult *Schistosoma bovis* worms. Proteomics.
635 2006;6 Suppl 1:S226-36.
- 636 9. Mathieson W, Wilson RA. A comparative proteomic study of the undeveloped and
637 developed *Schistosoma mansoni* egg and its contents: the miracidium, hatch fluid and secretions.
638 Int J Parasitol. 2010;40(5):617-28.
- 639 10. Cass CL, Johnson JR, Califf LL, Xu T, Hernandez HJ, Stadecker MJ, et al. Proteomic
640 analysis of *Schistosoma mansoni* egg secretions. Mol Biochem Parasitol. 2007;155(2):84-93.
- 641 11. Curwen RS, Ashton PD, Johnston DA, Wilson RA. The *Schistosoma mansoni* soluble
642 proteome: a comparison across four life-cycle stages. Mol Biochem Parasitol. 2004;138(1):57-66.
- 643 12. Wilson RA. Proteomics at the schistosome-mammalian host interface: any prospects for
644 diagnostics or vaccines? Parasitology. 2012;139(9):1178-94.
- 645 13. Sotillo J, Pearson MS, Becker L, Mekonnen GG, Amoah AS, van Dam G, et al. In-depth
646 proteomic characterization of *Schistosoma haematobium*: Towards the development of new tools
647 for elimination. PLoS Negl Trop Dis. 2019;13(5):e0007362.

- 648 14. Sotillo J, Pearson M, Potriquet J, Becker L, Pickering D, Mulvenna J, et al. Extracellular
649 vesicles secreted by *Schistosoma mansoni* contain protein vaccine candidates. *Int J Parasitol.*
650 2016;46(1):1-5.
- 651 15. Samoil V, Dagenais M, Ganapathy V, Aldridge J, Glebov A, Jardim A, et al. Vesicle-based
652 secretion in schistosomes: Analysis of protein and microRNA (miRNA) content of exosome-like
653 vesicles derived from *Schistosoma mansoni*. *Sci Rep.* 2018;8(1):3286.
- 654 16. Wang L, Li Z, Shen J, Liu Z, Liang J, Wu X, et al. Exosome-like vesicles derived by
655 *Schistosoma japonicum* adult worms mediates M1 type immune-activity of macrophage. *Parasitol*
656 *Res.* 2015;114(5):1865-73.
- 657 17. Zhu L, Liu J, Dao J, Lu K, Li H, Gu H, et al. Molecular characterization of *S. japonicum*
658 exosome-like vesicles reveals their regulatory roles in parasite-host interactions. *Sci Rep.*
659 2016;6:25885.
- 660 18. Zhu S, Wang S, Lin Y, Jiang P, Cui X, Wang X, et al. Release of extracellular vesicles
661 containing small RNAs from the eggs of *Schistosoma japonicum*. *Parasit Vectors.* 2016;9(1):574.
- 662 19. van Niel G, D'Angelo G, Raposo G. Shedding light on the cell biology of extracellular
663 vesicles. *Nat Rev Mol Cell Biol.* 2018;19:213.
- 664 20. Colombo M, Raposo G, Thery C. Biogenesis, secretion, and intercellular interactions of
665 exosomes and other extracellular vesicles. *Annu Rev Cell Dev Biol.* 2014;30:255-89.
- 666 21. Buck AH, Coakley G, Simbari F, McSorley HJ, Quintana JF, Le Bihan T, et al. Exosomes
667 secreted by nematode parasites transfer small RNAs to mammalian cells and modulate innate
668 immunity. *Nat Commun.* 2014;5:5488.
- 669 22. Trelis M, Galiano A, Bolado A, Toledo R, Marcilla A, Bernal D. Subcutaneous injection of
670 exosomes reduces symptom severity and mortality induced by *Echinostoma caproni* infection in
671 BALB/c mice. *Int J Parasitol.* 2016;46(12):799-808.
- 672 23. Chaiyadet S, Sotillo J, Krueajampa W, Thongsen S, Brindley PJ, Sripa B, et al.
673 Vaccination of hamsters with *Opisthorchis viverrini* extracellular vesicles and vesicle-derived
674 recombinant tetraspanins induces antibodies that block vesicle uptake by cholangiocytes and
675 reduce parasite burden after challenge infection. *PLOS Neglect Trop D.* 2019;13(5):e0007450.

- 676 24. Tucker MS, Karunaratne LB, Lewis FA, Freitas TC, Liang YS. Schistosomiasis. Curr
677 Protoc Immunol. 2013;103:Unit 19 1.
- 678 25. Basch PF. Establishment of cultures from cercariae and development until pairing. J
679 Parasitol. 1981;67:179–85.
- 680 26. Webber J, Clayton A. How pure are your vesicles? J Extracell Vesicles. 2013;2.
- 681 27. Robinson MW, Buchtman KA, Jenkins C, Tacchi JL, Raymond BB, To J, et al.
682 MHJ_0125 is an M42 glutamyl aminopeptidase that moonlights as a multifunctional adhesin on the
683 surface of *Mycoplasma hyopneumoniae*. Open Biol. 2013;3(4):130017.
- 684 28. Sotillo J, Sanchez-Flores A, Cantacessi C, Harcus Y, Pickering D, Bouchery T, et al.
685 Secreted proteomes of different developmental stages of the gastrointestinal nematode
686 *Nippostrongylus brasiliensis*. Mol cell proteomics. 2014;13(10):2736-51.
- 687 29. Milac TI, Randolph TW, Wang P. Analyzing LC-MS/MS data by spectral count and ion
688 abundance: two case studies. Stat Interface. 2012;5(1):75-87.
- 689 30. Conesa A, Gotz S, Garcia-Gomez JM, Terol J, Talon M, Robles M. Blast2GO: a universal
690 tool for annotation, visualization and analysis in functional genomics research. Bioinformatics.
691 2005;21(18):3674-6.
- 692 31. Supek F, Bošnjak M, Škunca N, Šmuc T. REVIGO summarizes and visualizes long lists of
693 gene ontology terms. PLoS One. 2011;6(7):e21800.
- 694 32. Emanuelsson O, Brunak S, von Heijne G, Nielsen H. Locating proteins in the cell using
695 TargetP, SignalP and related tools. Nat Protoc. 2007;2(4):953-71.
- 696 33. Krogh A, Larsson B, von Heijne G, Sonnhammer EL. Predicting transmembrane protein
697 topology with a hidden Markov model: application to complete genomes. J Mol Biol.
698 2001;305(3):567-80.
- 699 34. Eichenberger RM, Ryan S, Jones L, Buitrago G, Polster R, Montes de Oca M, et al.
700 Hookworm secreted extracellular vesicles interact with host cells and prevent inducible colitis in
701 mice. Front Immunol. 2018;9(850).

- 702 35. Eichenberger RM, Talukder MH, Field MA, Wangchuk P, Giacomini P, Loukas A, et al.
703 Characterization of *Trichuris muris* secreted proteins and extracellular vesicles provides new
704 insights into host-parasite communication. *J Extracell Vesicles*. 2018;7(1):1428004.
- 705 36. Kalra H, Drummen GP, Mathivanan S. Focus on extracellular vesicles: Introducing the
706 next small big thing. *Int J Mol Sci*. 2016;17(2):170.
- 707 37. Théry C, Amigorena S, Raposo G, Clayton A. Isolation and characterization of exosomes
708 from cell culture supernatants and biological fluids. *Curr Protoc Cell Biol*. 2006;30(1):3.22.1-3.9.
- 709 38. Tauro BJ, Greening DW, Mathias RA, Mathivanan S, Ji H, Simpson RJ. Two distinct
710 populations of exosomes are released from LIM1863 colon carcinoma cell-derived organoids. *Mol*
711 *Cell Proteomics*. 2013;12(3):587-98.
- 712 39. Raposo G, Stoorvogel W. Extracellular vesicles: exosomes, microvesicles, and friends. *J*
713 *Cell Biol*. 2013;200(4):373-83.
- 714 40. Booth AM, Fang Y, Fallon JK, Yang J-M, Hildreth JEK, Gould SJ. Exosomes and HIV
715 Gag bud from endosome-like domains of the T cell plasma membrane. *J Cell Biol*.
716 2006;172(6):923-35.
- 717 41. Nowacki FC, Swain MT, Klychnikov OI, Niazi U, Ivens A, Quintana JF, et al. Protein and
718 small non-coding RNA-enriched extracellular vesicles are released by the pathogenic blood fluke
719 *Schistosoma mansoni*. *J Extracell Vesicles*. 2015;4:28665.
- 720 42. Marcilla A, Trelis M, Cortes A, Sotillo J, Cantalapiedra F, Minguéz MT, et al.
721 Extracellular vesicles from parasitic helminths contain specific excretory/secretory proteins and are
722 internalized in intestinal host cells. *PLoS One*. 2012;7(9):e45974.
- 723 43. Bernal D, Trelis M, Montaner S, Cantalapiedra F, Galiano A, Hackenberg M, et al. Surface
724 analysis of *Dicrocoelium dendriticum*. The molecular characterization of exosomes reveals the
725 presence of miRNAs. *J Proteomics*. 2014;105:232-41.
- 726 44. Cwiklinski K, de la Torre-Escudero E, Trelis M, Bernal D, Dufresne PJ, Brennan GP, et al.
727 The extracellular vesicles of the helminth pathogen, *Fasciola hepatica*: biogenesis pathways and
728 cargo molecules involved in parasite pathogenesis. *Mol Cell Proteomics*. 2015;14(12):3258-73.

- 729 45. Chaiyadet S, Smout M, Johnson M, Whitchurch C, Turnbull L, Kaewkes S, et al.
730 Excretory/secretory products of the carcinogenic liver fluke are endocytosed by human
731 cholangiocytes and drive cell proliferation and IL6 production. *Int J Parasitol.* 2015;45(12):773-81.
- 732 46. Zamanian M, Fraser LM, Agbedanu PN, Harischandra H, Moorhead AR, Day TA, et al.
733 Release of small RNA-containing exosome-like vesicles from the human filarial parasite *Brugia*
734 *malayi*. *PLoS Negl Trop Dis.* 2015;9(9):e0004069.
- 735 47. Hansen EP, Kringel H, Williams AR, Nejsum P. Secretion of RNA-containing
736 extracellular vesicles by the porcine whipworm, *Trichuris suis*. *J Parasitol.* 2015;101(3):336-40.
- 737 48. Simbari F, McCaskill J, Coakley G, Millar M, Maizels RM, Fabriás G, et al. Plasmalogen
738 enrichment in exosomes secreted by a nematode parasite versus those derived from its mouse host:
739 implications for exosome stability and biology. *J Extracell Vesicles.* 2016;5:30741-.
- 740 49. Tzelos T, Matthews JB, Buck AH, Simbari F, Frew D, Inglis NF, et al. A preliminary
741 proteomic characterisation of extracellular vesicles released by the ovine parasitic nematode,
742 *Teladorsagia circumcincta*. *Vet Parasitol.* 2016;221:84-92.
- 743 50. Harischandra H, Yuan W, Loghry HJ, Zamanian M, Kimber MJ. Profiling extracellular
744 vesicle release by the filarial nematode *Brugia malayi* reveals sex-specific differences in cargo and
745 a sensitivity to ivermectin. *PLoS Negl Trop Dis.* 2018;12(4):e0006438.
- 746 51. Shears RK, Bancroft AJ, Hughes GW, Grecis RK, Thornton DJ. Extracellular vesicles
747 induce protective immunity against *Trichuris muris*. *Parasite Immunol.* 2018;40(7):e12536.
- 748 52. Siles-Lucas M, Sanchez-Ovejero C, Gonzalez-Sanchez M, Gonzalez E, Falcon-Perez JM,
749 Boufana B, et al. Isolation and characterization of exosomes derived from fertile sheep hydatid
750 cysts. *Vet Parasitol.* 2017;236:22-33.
- 751 53. Ancarola ME, Marcilla A, Herz M, Macchiaroli N, Perez M, Asurmendi S, et al. Cestode
752 parasites release extracellular vesicles with microRNAs and immunodiagnostic protein cargo. *Int J*
753 *Parasitol.* 2017;47(10-11):675-86.
- 754 54. Nicolao MC, Rodriguez Rodrigues C, Cumino AC. Extracellular vesicles from
755 *Echinococcus granulosus* larval stage: Isolation, characterization and uptake by dendritic cells.
756 *PLoS Negl Trop Dis.* 2019;13(1):e0007032.

- 757 55. Tendler M, Brito CA, Vilar MM, Serra-Freire N, Diogo CM, Almeida MS, et al. A
758 *Schistosoma mansoni* fatty acid-binding protein, Sm14, is the potential basis of a dual-purpose anti-
759 helminth vaccine. Proc Natl Acad Sci U S A. 1996;93(1):269-73.
- 760 56. Macalanda AMC, Angeles JMM, Moendeg KJ, Dang AT, Higuchi L, Inoue N, et al.
761 Evaluation of *Schistosoma japonicum* thioredoxin peroxidase-1 as a potential circulating antigen
762 target for the diagnosis of Asian schistosomiasis. J Vet Med Sci. 2018;80(1):156-63.
- 763 57. Bourke CD, Nausch N, Rujeni N, Appleby LJ, Trottein F, Midzi N, et al. Cytokine
764 responses to the anti-schistosome vaccine candidate antigen glutathione-S-transferase vary with
765 host age and are boosted by praziquantel treatment. PLoS Negl Trop Dis. 2014;8(5):e2846.
- 766 58. Boulanger D, Reid GD, Sturrock RF, Wolowczuk I, Balloul JM, Grezel D, et al.
767 Immunization of mice and baboons with the recombinant Sm28GST affects both worm viability
768 and fecundity after experimental infection with *Schistosoma mansoni*. Parasite Immunol.
769 1991;13(5):473-90.
- 770 59. Hoffmann KF, Strand M. Molecular identification of a *Schistosoma mansoni* tegumental
771 protein with similarity to cytoplasmic dynein light chains. J Biol Chem. 1996;271(42):26117-23.
- 772 60. Tebeje BM, Harvie M, You H, Loukas A, McManus DP. Schistosomiasis vaccines: where
773 do we stand? Parasit Vectors. 2016;9(1):528.
- 774 61. Sanderson RD, Bandari SK, Vlodaysky I. Proteases and glycosidases on the surface of
775 exosomes: Newly discovered mechanisms for extracellular remodeling. Matrix Biol. 2019;75-
776 76:160-9.
- 777 62. Shimoda M, Khokha R. Metalloproteinases in extracellular vesicles. Biochim Biophys
778 Acta Mol Cell Res. 2017;1864(11 Pt A):1989-2000.
- 779 63. Silva LL, Marcet-Houben M, Zerlotini A, Gabaldon T, Oliveira G, Nahum LA.
780 Evolutionary histories of expanded peptidase families in *Schistosoma mansoni*. Mem Inst Oswaldo
781 Cruz. 2011;106(7):864-77.
- 782 64. Caffrey CR, Goupil L, Rebello KM, Dalton JP, Smith D. Cysteine proteases as digestive
783 enzymes in parasitic helminths. PLoS Negl Trop Dis. 2018;12(8):e0005840.

- 784 65. Mathivanan S, Ji H, Simpson RJ. Exosomes: Extracellular organelles important in
785 intercellular communication. *J Proteomics*. 2010;73(10):1907-20.
- 786 66. Simpson RJ, Kalra H, Mathivanan S. ExoCarta as a resource for exosomal research. *J*
787 *Extracell Vesicles*. 2012;1.
- 788 67. Crescitelli R, Lasser C, Szabo TG, Kittel A, Eldh M, Dianzani I, et al. Distinct RNA
789 profiles in subpopulations of extracellular vesicles: apoptotic bodies, microvesicles and exosomes.
790 *J Extracell Vesicles*. 2013;2.
- 791 68. Kowal J, Arras G, Colombo M, Jouve M, Morath JP, Primdal-Bengtson B, et al. Proteomic
792 comparison defines novel markers to characterize heterogeneous populations of extracellular
793 vesicle subtypes. *Proc Natl Acad Sci U S A*. 2016;113(8):E968-77.
- 794 69. Jeppesen DK, Fenix AM, Franklin JL, Higginbotham JN, Zhang Q, Zimmerman LJ, et al.
795 Reassessment of exosome composition. *Cell*. 2019;177(2):428-45.e18.
- 796 70. Lenassi M, Cagney G, Liao M, Vaupotic T, Bartholomeeusen K, Cheng Y, et al. HIV Nef
797 is secreted in exosomes and triggers apoptosis in bystander CD4+ T cells. *Traffic*. 2010;11(1):110-
798 22.
- 799 71. Fang Y, Wu N, Gan X, Yan W, Morrell JC, Gould SJ. Higher-order oligomerization targets
800 plasma membrane proteins and HIV gag to exosomes. *PLoS Biol*. 2007;5(6):e158-e.
- 801 72. Tran MH, Pearson MS, Bethony JM, Smyth DJ, Jones MK, Duke M, et al. Tetraspanins on
802 the surface of *Schistosoma mansoni* are protective antigens against schistosomiasis. *Nat Med*.
803 2006;12(7):835-40.
- 804 73. Bergquist R, Al-Sherbiny M, Barakat R, Olds R. Blueprint for schistosomiasis vaccine
805 development. *Acta Trop*. 2002;82(2):183-92.
- 806 74. Capron A, Capron M, Dombrowicz D, Riveau G. Vaccine strategies against
807 schistosomiasis: from concepts to clinical trials. *Int Arch Allergy Immunol*. 2001;124(1-3):9-15.
- 808 75. Cardoso FC, Pacifico RN, Mortara RA, Oliveira SC. Human antibody responses of patients
809 living in endemic areas for schistosomiasis to the tegumental protein Sm29 identified through
810 genomic studies. *Clin Exp Immunol*. 2006;144(3):382-91.

- 811 76. Jankovic D, Aslund L, Oswald IP, Caspar P, Champion C, Pearce E, et al. Calpain is the
812 target antigen of a Th1 clone that transfers protective immunity against *Schistosoma mansoni*. J
813 Immunol. 1996;157(2):806-14.
- 814 77. Le L, Alam MU, Zhang W, Karmakar S, Siddiqui AA, Ahmad G, et al. Use of an Sm-p80–
815 based therapeutic vaccine to kill established adult schistosome parasites in chronically infected
816 baboons. J Infect Dis. 2014;209(12):1929-40.
- 817 78. Karmakar S, Zhang W, Ahmad G, Torben W, Alam MU, Le L, et al. Use of an Sm-p80-
818 based therapeutic vaccine to kill established adult schistosome parasites in chronically infected
819 baboons. J Infect Dis. 2014;209(12):1929-40.
- 820 79. Krautz-Peterson G, Debatis M, Tremblay JM, Oliveira SC, Da'dara AA, Skelly PJ, et al.
821 *Schistosoma mansoni* infection of mice, rats and humans elicits a strong antibody response to a
822 limited number of reduction-sensitive epitopes on five major tegumental membrane proteins. PLoS
823 Negl Trop Dis. 2017;11(1):e0005306.
- 824 80. Han Z-G, Brindley PJ, Wang S-Y, Chen Z. Schistosoma genomics: new perspectives on
825 schistosome biology and host-parasite interaction. Ann Rev Genomics Hum Genet. 2009;10:211-
826 40.
- 827 81. Salzet M, Capron A, Stefano GB. Molecular crosstalk in host-parasite relationships:
828 schistosome- and leech-host interactions. Parasitol Today. 2000;16(12):536-40.
- 829 82. Chaiyadet S, Sotillo J, Smout M, Cantacessi C, Jones MK, Johnson MS, et al.
830 Carcinogenic liver fluke secretes extracellular vesicles that promote cholangiocytes to adopt a
831 tumorigenic phenotype. J Infect Dis. 2015;212(10):1636-45.
- 832 83. D'Acquisto F, Perretti M, Flower RJ. Annexin-A1: a pivotal regulator of the innate and
833 adaptive immune systems. Br J Pharmacol. 2008;155(2):152-69.
- 834 84. Madureira PA, Surette AP, Phipps KD, Taboski MAS, Miller VA, Waisman DM. The role
835 of the annexin A2 heterotetramer in vascular fibrinolysis. Blood. 2011;118(18):4789-97.
- 836 85. Don TA, Bethony JM, Loukas A. Saposin-like proteins are expressed in the gastrodermis
837 of *Schistosoma mansoni* and are immunogenic in natural infections. Int J Infect Dis.
838 2008;12(6):e39-e47.

839 86. Figueiredo BC, Da'dara AA, Oliveira SC, Skelly PJ. Schistosomes enhance plasminogen
840 activation: The role of tegumental enolase. PLoS Pathog. 2015;11(12):e1005335.

841 87. Kowal J, Tkach M, Thery C. Biogenesis and secretion of exosomes. Curr Opin Cell Biol.
842 2014;29:116-25.

843 88. Hyenne V, Labouesse M, Goetz JG. The Small GTPase Ral orchestrates MVB biogenesis
844 and exosome secretion. Small GTPases. 2018;9(6):445-51.

845 89. de la Torre-Escudero E, Gerlach JQ, Bennett APS, Cwiklinski K, Jewhurst HL, Huson
846 KM, et al. Surface molecules of extracellular vesicles secreted by the helminth pathogen *Fasciola*
847 *hepatica* direct their internalisation by host cells. PLoS Negl Trop Dis. 2019;13(1):e0007087.

848 90. Zhao C, Sun X, Li L. Biogenesis and function of extracellular miRNAs. ExRNA.
849 2019;1(1):38.

850 91. Stenmark H. Rab GTPases as coordinators of vesicle traffic. Nat Rev Mol Cell Biol.
851 2009;10(8):513-25.

852

853

854 **Appendix. SUPPLEMENTARY DATA**

855 **Supplementary Table 1.** Surface-exposed proteins released by trypsin treatment of
856 *Schistosoma mansoni*-derived 120k pellet vesicles.

857 **Supplementary Table 2.** Intra-vesicular cargo proteins identified after lysis of
858 *Schistosoma mansoni*-derived 120k pellet vesicles.

859 **Supplementary Table 3.** Integral membrane proteins from *Schistosoma mansoni*-derived
860 120k pellet vesicles.

861 **Supplementary Table 4.** Peripheral membrane proteins proteins from *Schistosoma*
862 *mansoni*-derived 120k pellet vesicles.

863 **Supplementary Table 5.** Surface-exposed proteins released by trypsin treatment of
864 *Schistosoma mansoni*-derived 15k pellet vesicles.

865 **Supplementary Table 6.** Intra-vesicular cargo proteins identified after lysis of
866 *Schistosoma mansoni*-derived 15k pellet vesicles.

867 **Supplementary Table 7.** Integral membrane proteins from *Schistosoma mansoni*-derived
868 15k pellet vesicles.

869 **Supplementary Table 8.** Peripheral membrane proteins proteins from *Schistosoma*
870 *mansoni*-derived 15k pellet vesicles.

871 **Supplementary Table 9.** Protein families identified from *Schistosoma mansoni*-derived
872 120k pellet vesicles.

873 **Supplementary Table 10.** Protein families identified from *Schistosoma mansoni*-derived
874 15k pellet vesicles.

875 **Supplementary Table 11.** Signal peptide predictions for proteins identified from

876 *Schistosoma mansoni*-derived 120k pellet vesicles.

877 **Supplementary Table 12.** Signal peptide predictions for proteins identified from

878 *Schistosoma mansoni*-derived 15k pellet vesicles.

879 **Supplementary Table 13.** Transmembrane domain predictions for proteins identified from

880 *Schistosoma mansoni*-derived 120k pellet vesicles.

881 **Supplementary Table 14.** Transmembrane domain predictions for proteins identified from

882 *Schistosoma mansoni*-derived 15k pellet vesicles.